MODIFICATION OF TITANIUM DIOXIDE NANOPARTICLE TO ENHANCE THE PHOTOACTIVITY IN VISIBLE LIGHT REGION

TAN WOOI CHUAN

BACHELOR OF CHEMICAL ENGINEERING
UNIVERSITI MALAYSIA PAHANG

Thesis Access Form

No_____Location_____

Author : ……

Title : ……

Status of access OPEN / RESTRICTED / CONFIDENTIAL

Moratorium period:_____ years, ending_____/_____200____

Conditions of access proved by (CAPITALS): ASSOC PROF MD DR MAKSUDUR RAHMAN KHAN

Supervisor (Signature)……

Faculty: ……

Author's Declaration: *I agree the following conditions:*

OPEN access work shall be made available (in the University and externally) and reproduced as necessary at the discretion of the University Librarian or Head of Department. It may also be copied by the British Library in microfilm or other form for supply to requesting libraries or individuals, subject to an indication of intended use for non-publishing purposes in the following form, placed on the copy and on any covering document or label.

*The statement itself shall apply to **ALL** copies:*

This copy has been supplied on the understanding that it is copyright material and that no quotation from the thesis may be published without proper acknowledgement.

Restricted/confidential work: All access and any photocopying shall be strictly subject to written permission from the University Head of Department and any external sponsor, if any.

Author's signature…….Date: ……

users declaration: for signature during any Moratorium period (Not Open work):
I undertake to uphold the above conditions:

Date	Name (CAPITALS)	Signature	Address

MODIFICATION OF TITANIUM DIOXIDE NANOPARTICLE TO ENHANCE THE PHOTOACTIVITY IN VISIBLE LIGHT REGION

TAN WOOI CHUAN

Thesis submitted in partial fulfilment of the requirements
for the award of the degree of
Bachelor of Chemical Engineering

Faculty of Chemical & Natural Resources Engineering
UNIVERSITI MALAYSIA PAHANG

JULY 2013

SUPERVISOR'S DECLARATION

We hereby declare that we have checked this thesis and in our opinion, this thesis is adequate in terms of scope and quality for the award of the degree of Bachelor of Chemical Engineering.

Signature :
Name of main supervisor : ASSOC PROF MD DR MAKSUDUR RAHMAN KHAN
Position : SENIOR LECTURER
Date : 4 JULY 2013

STUDENT'S DECLARATION

I hereby declare that the work in this thesis is my own except for quotations and summaries which have been duly acknowledged. The thesis has not been accepted for any degree and is not concurrently submitted for award of other degree.

Signature :
Name : TAN WOOI CHUAN
ID Number : KA09065
Date : JULY 2013

DEDICATION

This thesis is dedicated to my parents

For their sempiternal support and encouragement all the time in my life

To my brothers

For being with me all the time when there is no one else around

To my supervisor

For the faith and trust that he had put upon me for the project

ACKNOWLEDGEMENT

First and foremost, I would like to express my utmost gratitude to my parents Tan Keng Kiang and Cheah Pek Kwan for their endless support and encouragement physical and mentally especially when I'm in my depressing period during the my time in my university. The support given during the period has bringing a new strength and making me a better person for my future.

Secondly, I would like to express my utmost gratitude to my brother Tan Wooi Phang, Tan Wooi Yang, Matthew Lim Yew Phei and Kwan Soon Cheong for being with me all the time when I'm needed all the time. Although I have lost my aim and myself during these times, all of you are willing to share your precious time to listen out to me and share your wise knowledge and experience on the philosophy in life and this world is priceless. The time spent during these days with all of you has been great, where the moment that we spent has been a great momentum for me to complete the thesis.

Thirdly, I would like to express my utmost gratitude to my supervisor, Assoc. Prof. Md. Dr. Maksudur Rahman Khan. The faith and trust that he entrusted to me is cannot be conveyed by a mere statement. Thank you for being able to continue to trust me although I'm not able to meet up your expectation towards me. Thank you, thank you, and thank you again for believing me again although I'm just a good for nothing people who still have a long way to go to be a more mature and bears a larger responsibility for anything.

Not to forget also an utmost gratitude to all my friends and colleague in university, Leong Sheng Yau, Ong Hong Ruey, Balanitharan, Amalina, Hamidah and etc for the willingness to share your knowledge all this time. Not to forget also those that who I encountered during this time such as Nazir and Anila from UKM, Dr Angelina from University of Nottingham, Dr Guru from Faculty of Industrial Science and Technology, all the technician in the chemical lab, and all others people that I meet along during my time in the university.

"Thank you for every happening that giving me courage to complete this thesis and to make me and people around me to be a better person in future"

ABSTRACT

In recent year, photocatalyst has been gaining a wide attention as the ability to harness the free energy from sunlight to perform variety of function such as organic degradation, solar cell and etc. When used as photocatalyst, titanium dioxide (TiO_2) is able to absorb ultraviolet light only (UV) to initiate the oxidation and reduction which is able to speed up the degradation of dye. This thus provides a cheap and efficient method to solve the dye mismanagement that is face in industries these days. In this work, the titanium dioxide nanoparticle is modified via hydrazine wet method to increase photocatalytic activity. The photocatalytic activity is studied via methylene blue degradation, followed by the kinetic study on the methylene blue degradation. The catalyst has been characterized via UV-VIS spectrophotometer, FTIR machine and XRD machine. From the result, we realized that the main reaction that occurred during the modification is combustion of hydrazine on the surface of TiO_2. From the UV-Vis spectrum, we found out that the modify catalyst can absorb more visible light as compare to the commercial TiO_2. FTIR spectrum indicated that NH_x group, NO group and an increase of OH group is presented after the modification. XRD pattern analysis suggested the crystallinity of the catalyst is slightly increased after the modification. Methylene blue degradation also showed that the modified catalyst have a higher activity as compared to the commercial one. The results obtained suggesting that the photocatalytic activity is increasing due to the ability of the catalyst to absorb visible light after the treatment. The modeling is done by relating the rate of methylene blue degradation with the direct hole attack and the hydroxyl radical attack occurred in the reaction.

ABSTRAK

Di kian hari, keupayaan fotokatalis untuk mempergunakan tanaga matahari untuk melakukan pelbagai aktiviti seperti degradasi pewarna, sel solar dan sebagainya telah menerima perhatian dari pelbagai pihak. Apabila digunakan sebagai fotokatalis, TiO_2 dapat menyerap tenaga cahaya ultraungu (UV) untuk memulakan proses pengoksidaan dan reduksi, di mana prosess ini adalah berfaedah untuk mempercepatkan prosess degradasi pewarna. Keupayaan ini telah menyumbangkan idea untuk menyelesaikan masalah pengendalian pewarna yang dihadapi oleh pihak industri baru-baru ini. Dalam kertas ini, TiO_2 telah dimodifikasi mengunakan teknik kebasahan hydrazin untuk meningkatkan fotoaktiviti pemangkin tersebut. Fotoaktivi pemangkin adalah dikaji melaui degradasi biru metilena, diikuti oleh kajian kinetik terhadap reaksi tersebut. Sifat-sifat pemangkin adalah diperoleh melalui spektrofotometer UV-VIS, mesin FTIR dan mesin XRD. Melaui eksperiment, ianya didapati bahawa reaksi yang berlaku semasa modikasi berlaku adalah pembakaran hydrazin di atas permukaan TiO_2. Melalui keputusan yang diperoleh, pemangkin yang dimodifikasi berupaya untuk menyerap lebih banyak cahaya ketara berbanding dengan pemangkin komersial. Spektrum FTIR mencadamgkan kumpulan NH_x dan NO, diikuti oleh penambahan kumpulan OH telah muncul di atas pemangkin selepas berlakunya modifikasi. Spektra XRD juga menunjukan peningkatan kristaliniti dalam pemangkin selepas berlakunya modifikasi. Ujian degradasi biru metilena juga menunjukan pemangkin yang dimodifikasi menunjukkan fotoaktiviti yang tinggi berbanding pemangkin komersial. Keputusan ini telah menunjukan terdapat peningkatan fotoaktiviti dalam pemangkin yang telah dimodifikasi adalah disebabkan oleh keupayaan pemangkin untuk menyarap cahaya ketara selepas dimodifikasi. Pemodalan reaksi telah dibuat dengan mengaitkan kadar degradasi biru metilena dengan serangan lubang berketerusan dan serangan hidroksil radikal yang berlaku dalam reaksi tersebut.

TABLE OF CONTENT

SUPERVISOR'S DECLARATION IV
STUDENT'S DECLARATION V
DEDICATION VI
ACKNOWLEDGEMENT VII
ABSTRACT IX
ABSTRAK X
TABLE OF CONTENT XI
LIST OF FIGURES XIII
LIST OF TABLES XV
LIST OF ABBREVIATIONS XVI
1 INTRODUCTION 1
1.1 Overview 1
1.2 Background of the Proposed Study 2
1.3 Problem Statements 3
1.4 Research Objective 3
1.5 Research Question/ Hypotheses 4
1.6 Scope 4
1.7 Expected Outcome 5
1.8 Significance of the Proposed Study 5
2 LITERATURE REVIEW 6
2.1 Introduction 6
2.2 Ti^{3+} Defect Site, Oxygen Vacancy and Surface Disordered Layer 6
2.3 Nitrogen Doping TiO_2 9
2.4 Hydrazine Wet Method 11
2.4.1 Interaction of Hydrazine with TiO_2 13
2.5 Methylene Blue Degradation Modeling 14
3 METHODOLOGY 18
3.1 Introduction 18
3.1.1 Catalyst Preparation 18
3.1.2 Materials and Equipment 19
3.1.3 Procedure 19

3.2 Photoactivity Test Measurement 20
3.2.1 Materials and Equipment 21
3.2.2 Procedure 22
3.2.2.1 Stock Solution Preparation 22
3.2.2.2 Calibration Curve 22
3.2.2.3 Photoactivity Reaction 23
3.2.2.4 Methylene Blue Concentration Measurement 25
3.3 Catalyst Characterization 26
3.4 Kinetic Studies 27
4 RESULT AND DISCUSSION 28
4.1 Introduction 28
4.2 UV-Vis Absorption Spectra Analysis 28
4.3 FTIR Analysis 32
4.4 XRD Analysis 33
4.5 Methylene Blue Degradation 36
4.6 Kinetic Studies 40
5 CONCLUSION AND RECOMMENDATION 48
5.1 Conclusion 48
5.2 Recommendation 49
REFERENCES 51
APPENDICES A-1
TECHINCAL PAPER A-2

LIST OF FIGURES

Figure 1.1: Schematic diagram on photoexcitaion and the deexcitation phenomena in photocatalyst (Linsebigler et al, 1995) 2

Figure 2.1: Formation of mid gap at forbidden band gap caused by Ti-O-N and chemisorb N in TiO_2 (Viswanathan et al, 2012). 10

Figure 2.2: The reaction pathway of atoms as described by Langmuir-Hinshelwood mechanism rate law. 16

Figure 2.3: Graph of rate of methylene blue degradation vs concentration of methylene blue from Sannio et al (2013) data 17

Figure 3.1: Black Box 24

Figure 3.2: Set up of high intensity lamp, water cooling system, jacketed batch reactor and the mixing plate in the black box 24

Figure 4.1: Color of the catalyst after the wet hydrazine treatment. From left: commercial TiO_2, N-TiO_2-60, N-TiO_2-110, and N-TiO_2-170. 29

Figure 4.2: Absorbance spectra of the commercial TiO_2, N-TiO_2-60, N-TiO_2-110, and N-TiO_2-170. 31

Figure 4.3: FTIR spectra for the commercial TiO_2 and N-TiO_2-170 33

Figure 4.4: XRD Pattern for commercial TiO_2 and N-TiO_2-170 34

Figure 4.5: Calibration curve between concentration of the methylene blue and the absorbance height 36

Figure 4.6: UV-Vis spectra for methylene blue collected from reaction with commercial TiO_2 at various time 37

Figure 4.7: UV-Vis spectra for methylene blue collected from reaction with N-TiO_2-170 at various time 38

Figure 4.8: Degradation of methylene blue with commercial TiO_2 and N-TiO_2-170; Initial methylene blue concentration: 50ppm; Weight of catalyst: 0.01g 39

Figure 4.9: Graph of rate of methylene blue (MB) degradation over time 46

Figure 4.10: Graph of -1/rate of methylene blue degradation versus the 1/concentration of the methylene blue 47

LIST OF TABLES

Table 4.1: The concentration of the methylene blue (MB) along the reaction time from reaction with commercial TiO_2 37

Table 4.2: The concentration of the methylene blue (MB) along the reaction time from reaction with N-TiO_2-170..... 38

Table A.1: Peak List for the commercial TiO_2 from XRD analysis A-1

Table A.2: Peak List for the N-TiO_2-170 from XRD analysis..... A-1

LIST OF ABBREVIATIONS

Abbreviation	*Definition*
N-TiO2-60	Commercial catalyst treated at 60˚C
N-TiO2-110	Commercial catalyst treated at 110˚C
N-TiO2-170	Commercial catalyst treated at 170˚C
XRD	X-Ray Diffraction
FTIR	Fourier Transform Infra-Red
UV-Vis	Ultraviolet/Visible
MB	Methylene Blue
XPS	X-ray Photoelectron Spectroscopy
QSSA	Quasi Steady State Assumption

1 INTRODUCTION

1.1 Overview

Photo-catalyst is one of a kind catalyst which utilizing light to play a part in modify the rates of photo-reaction. Photo-catalyst has the ability to initiate oxidation and reduction process when the light is illuminated on the surface of the catalyst due to the existence of the band gap in the semiconductor, which differ them from the normal catalyst which depending on the adsorption, surface reaction and the desorption of the surrounding molecule to improve rate of reaction. When the electron in the valance band has absorbed photon from a particular wavelength, the electron in the valance band will be excited to the conduction band, leaving a hole in the valance band. Later on, the electrons on the conduction band will move to surface of the catalyst to initiate reduction process, while the holes at the valance band will move to surface to initiate oxidation process. So far semiconductor like TiO_2 is proven better in terms of cost, stability and performance compare to other semiconductor, still the large band gap in TiO_2 (3.2eV) causing the catalyst can absorb only UV light and only can work in near UV range visible light only (Jiang et al, 2012). This cause the application of TiO2 inconvenient and costly as another UV source is needed to enable the function of TiO_2. At the same time, sunlight at the top of Earth's atmosphere consisted of about 50% infrared light, 40% visible light and 10% UV light (Qiang Fu, 2003). So it is desired that TiO_2 is modified to be able to absorb those lights from the sun itself.

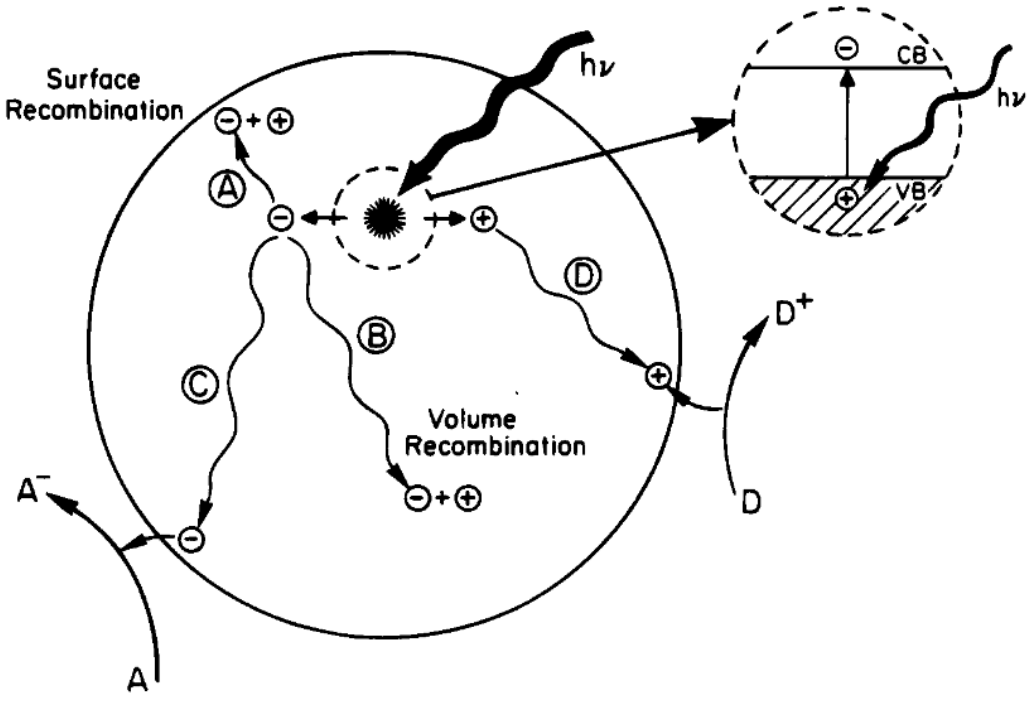

Figure 1.1: Schematic diagram on photoexcitaion and the deexcitation phenomena in photocatalyst (Linsebigler et al, 1995)

1.2 Background of the Proposed Study

Large amounts of colored wastewater are generated in industries which use dye such as methylene blue to give the desired color to their product. Still these dye is mismanaged and has been discharged into environment especially river without adequate control, resulting negative impact to the environment and to the human health (Zolinger et al, 1991). The presence of dye in in the natural stream can harm the aquatic life by increasing the toxicity and chemical oxygen demand, and impeding photosynthetic phenomena through reduction of light penetration (Bulut et al, 2006). So far, methods that are used to treat the dye are adsorption, electrocoagulation, ultrasonic decomposition, advance chemical oxidation, nanofiltration, and chemical coagulation followed by sedimentation were implemented to remove dyes from wastewater (Sannino et al, 2013). In recent year photocatalytic degradation with TiO_2 under visible light is gaining more attention in industry and academic. This is so as this method of treatment is much cost effective

as compared to method that is used currently; where sophisticated equipment is to be used in order to treat the dye. While with the proposed method, only few things are needed for the treatment: a reactor, a mixer, the catalyst and the sunlight.

1.3 Problem Statements

In order to create the TiO_2 that is much more active in visible light, one method that is studied the most so far is doping nitrogen into the lattice of TiO_2. So far there are various ways to dope the nitrogen into the lattice of TiO_2 such as sol-gel method, reaction of TiO_2 with N- containing species such as ammonia, urea and etc, plasma treatment method, and oxidation of Ti-N film to TiO_2-N film. Still usually all these methods is not cost effective for bulk production as the preparation usually involving sophisticated equipment and high temperature, especially the plasma treatment method involving creation of nitrogen in plasma form at temperature at 400˚C in a plasma chamber (Chen et al, 2007).

So far, wet hydrazine treatment method has been showing a promising way to prepare an N-doped TiO_2 (Li et al, 2007; Selvam et al, 2012). The modification process is done where the TiO_2 powder is immersed in hydrazine hydrate (80%) for 12 hour, filtered and dried with air at 110˚C. The simplicity of the process, the unnecessary of using harsh condition, and the needless of calcination making this treatment interesting as it is possible to convert the lab scale production of this catalyst to a larger scale with a minimum cost. Still the reaction that is occurred during the modification is still not fully understood.

1.4 Research Objective

The objective of the research is:

1) To synthesis N-TiO_2 that absorbs light in visible region using wet hydrazine method.

2) To inspect the photoactivity of the modified TiO2.

3) To model the methylene blue degradation reaction.

1.5 Research Question/ Hypotheses

Q1 What is the reaction involved in the wet hydrazine method?

H1 Hydrazine is an active chemical which can be burned at air at relative low temperature with a strong heat release (621.74kJ/mol) (Rane et al, 2007). It is speculated that ignitability of the hydrazine is the one that responsible for the nitrogen to be doped into the TiO_2 (Li et al, 2007). This speculated is associated with Li et al (2007) and Selvam et al (2012) respectively when a glow is actually detected on the surface of the catalyst when the TiO_2 and the hydrazine hydrate (80%) mixture is dried in air at 110˚C, turning the color of the catalyst from white to yellow color. So we hypothesize that the reaction that happened during the drying process is the combustion process. Still the exact temperature of the combustion to happen is still remaining unknown.

Q2 Is there another reaction happened between TiO_2 and hydrazine?

H2 According to Chung et al studies in 2000, it is found out that at 35˚C, an isolated hydroxyl group and several nitrogen species is bonded on TiO_2 when the gas hydrazine is exposed on the surface of TiO_2. When the temperature is increasing to 150˚C, the isolated hydroxyl group is decreasing along with the increment of temperature. But when the temperature is raised from 150˚C to 200˚C, the N_2H_4 adsorbed on the TiO_2 is further decompose to other N species or desorbed from the catalyst. At the same time the isolated hydroxyl adsorption in the range 3600-3800cm^{-1} is further enhanced along with this increment of temperature in this range. So with this, we can hypothesize that during the mixing, there is another reaction indeed happened besides the combustion of hydrazine as mentioned above.

1.6 Scope

This research will be focused on examine the effect of the drying temperature towards the catalyst itself. The effects that are concern is the properties of the catalyst such as the light absorption, phase of catalyst, species presented in the

catalyst, and the photocatalytic activity of the catalyst itself. For light absorption of the catalyst, the properties will be studied using UV-Vis Spectrophotometer. For the phase of catalyst, it will be studied using X-Ray Diffraction Machine. As to determine the species presented in the catalyst, FTIR analysis is performed to infer the species appeared in the catalyst. As for the photocatalytic activity studies, the methylene blue degradation studies has been conducted to check the photoactivity of the catalyst itself. Besides that, the kinetic study on the methylene blue degradation for the after modified TiO_2 is examined also in this project.

1.7 Expected Outcome

The expected outcomes of the research are:

1) The nitrogen is successfully doped inside the TiO_2 lattice via hydrazine combustion.

2) The photocatalytic activity of the N-TiO_2 is increased compared to the commercial TiO_2 due to the increase of the visible light absorption of the N-TiO_2.

3) The modeling on the methylene blue degradation with the modified catalyst is done.

1.8 Significance of the Proposed Study

With this study, a simplified method to create the catalyst will be more understood, especially on the reaction involved during the procedure that responsible to the doping of the nitrogen into the catalyst. By understanding the reaction occurred during the treatment, the bulk production of the catalyst will be possible by identifying and minimizing several vital variable as to make the method to be cost effective. With the modeling on the modified catalyst is done, the design equation for the photocatalytic reactor is available, making the volume design of the photocatalytic reactor is possible.

2 LITERATURE REVIEW

2.1 Introduction

Photo-catalyst is one of a kind catalyst which utilizing light to play a part in speeding up the reaction by initiating oxidation and reduction process when the light is illuminated on the surface of the catalyst. TiO_2 is proven better in terms of cost, stability and performance compare to other semiconductor, still the large band gap in TiO_2 (3.2eV) causing the catalyst can absorb only UV light and only can work in near UV range visible light only (Jiang et al, 2012). This cause the application of TiO2 inconvenient and costly as another UV source is needed to enable the function of TiO_2. Up until now, most researches have been focused on reducing the band gap of the semiconductor, in hoping that by reducing the band gap, TiO_2 is able to absorb the light from the visible range, thus improving the photoactivity of the catalyst itself. Here several strategies on how to reduce the band gap of the TiO_2 has been reviewed such as the creation of Ti^{3+} defect site, oxygen vacancy, surface disordered layer, and nitrogen doping. Later on, the literature review is also done on the relation to be used in the modeling of the methylene blue degradation.

2.2 Ti^{3+} Defect Site, Oxygen Vacancy and Surface Disordered Layer

In 2011, Chen et al reported a disorder-engineered TiO_2 nano-crystal which able to produce hydrogen via water splitting under sunlight. In the work, the prepared catalyst made is annealed in a very rough condition of 200˚C with 20bar hydrogen for 5 days, results a black colored TiO_2. Wang et al (2011) work on treating TiO_2 nanowire with hydrogen gas is only able to improve the UV light absorption, but still unable to convert the photon to current under the incident wavelength above 430nm. Using Helium gas as the inert gas for thermal treatment at 400˚C for 3 hour for 3 phases of TiO_2, Liu et al (2012) also get a similar result where the UV light absorption is improve but not able to absorb light in visible region.

It has been acknowledged that thermal annealing can create a Ti^{3+} defect site, or oxygen vacancies on the TiO_2 surface (Lu et al, 1994). This also can be done by annealing in a reducing atmosphere where the oxidation is prevented by introducing inert gas like hydrogen and helium (Xiong et al, 2011). In Wang et al (2011) work, the photo-activity enhancement in the UV region can be attributed to the increased electron donor density which is left by oxygen vacancies. While in Liu et al (2012) work, the Ti^{3+} defect sites is functioned as reactive sites for the adsorption of reactants and allow the effective charge or hole transfer between the reactant and the surface of the semiconductor. Lu et al (1994) also mention similar things where the oxygen vacant at bridging-O site leaves two Ti^{3+} exposed, making TiO_2 surface more reactive than other oxides such as Al_2O_3 and SiO_2, and affecting the dissociative chemisorption of molecules such as H_2O, NH_3 and etc.

Oxygen vacancies are also being responsible for visible light absorption (Xiong et al, 2011). It is believed that oxygen vacancy creates surface states in the forbidden band gap with energy 0.75 to 1.18eV below the conduction band minimum of TiO_2 (Cronemeyer, 1959). Wang et al (2011) suggested that the visible light is possible due to the transitions from the TiO_2 valance band to the oxygen vacancy state, or from the oxygen vacancies states to the conduction band since both ways require less energy for excitation. Here they hypothesize that the reason why their photo-catalyst couldn't absorb visible light is due both oxygen vacancy state is well below the redox potential of H_2O/H_2. Another hypothesis proposed is that the electronic transition between localized vacancy state and the delocalized conduction band is not significance as the coupling between both states should be weak. Still no UV-is spectrophotometer is done to check whether the catalyst itself is able to absorb the visible light.

Zuo et al (2010), with the aim to create a Ti^{3+} photo-catalyst via combustion method is able to absorb incident wavelength up until 700nm and above and reducing water to hydrogen gas under incident light with wavelength 400nm and above. The formation of the Ti^{3+} in the bulk is verified by Electron Paramagnetic Resonance (EPR) spectra. From EPR and X-ray Photoelectron Spectroscopy (XPS) study also, they confirmed that the Ti^{3+} is presented in the bulk of the catalyst instead on the surface of the catalyst. The Plane-Wave Self-Consistent Field (PWscf)

simulation also reveals that a mini band is rising up closely below the conduction band minimum, which is in agreement with Cronemeyer (1959) findings. They also realize that the width of the vacancy band is directly proportional to the concentration of the vacancy too. The success of the absorption of visible and infrared light can be contributed by creating Ti^{3+} in the bulk TiO_2 rather than on the surface. If the Ti^{3+} is created on the surface, the surrounding oxygen will be absorbed by Ti^{3+}, eliminating the oxygen vacancy and hence the surface state in the band gap. Wei et al (2012) also created Ti^{3+} in the bulk TiO_2 via hydrogenation, reporting wavelength absorption up until 1800nm as verified by UV-is diffuse reflectance spectra, signifying the importance of Ti^{3+} in the bulk to enabling the function of Ti^{3+} to absorb sunlight.

Examining the work by Chen et al (2011), one obvious difference between their works and the others is the objective to create a disorder engineered TiO_2, with the TiO_2 Nano-crystal as the core and the highly disordered layer as the shell, instead of creating a Ti^{3+} based TiO_2. In his work, the role of the disordered layer is to create mid-gap states. Mid-gap states or band tail states can form a continuum extending to and overlapping with the conduction band edge and the valance band, hence narrowing the band gap from 3.3eV to 1.54eV. This narrowing enabling the photo-catalyst to absorb simulated solar light ranging from 550nm to 700nm in methylene blue solution. Naldoni et al (2012) also obtained a similar result by creating the crystalline core/ disordered shell TiO_2 where the band gap is narrowed from 3.25eV to 1.85eV. At the same time, they also found out that their catalyst containing Ti^{3+} in the bulk; possess two oxygen vacancy surface states, therefore contributing in light absorption in the same way as mentioned by Wang et al (2011).

In Chen et al (2011) works, they found out that after hydrogenation, one H atom is bonded to an O atom while another atom is bonded to a Ti atom. This suggests that the source of the black color TiO_2 and the formation of the disordered layer are due to the formation of this crystal structure on TiO_2. Similar findings also reported by Wei et al (2011), where the formation of the Ti-H and O-H is founded on the surface of the TiO_2, contributing to the band gap narrowing besides the formation of Ti^{3+} in the bulk catalyst.

Still, there seems to be no a parallel pattern on how this surface disorder are created so far. In Chen et al (2011) work, the as-prepared TiO_2 powder is calcinated at 500˚C for 6 hour to improve the crystallinity of TiO_2. Later on the TiO_2 is heat treated in the chamber by hydrogenation at 20bar at 200˚C for 5 days to obtain black TiO_2. In Naldoni et al (2012) work, the TiO_2 first is treated under vacuum and then heated at 200˚C under O_2 flow for 1 hr. After the sample is cooled to room temperature, the TiO_2 is reduced in 500˚C under H_2 flow in 1 hr to obtain black TiO_2. In Wei et al (2011) work, the as prepared TiO_2 is treated with hydrogen in 10bar pressure, at 200˚C for 2 hr, yielding a dark blue TiO_2. In Wang et al (2011) work, the as prepared TiO_2 nanowire were 1st annealed in air for 3 hr, followed by hydrogen treatment at various temperature (200˚C to 550˚C) for 30 minute. The TiO_2 is founded to turn black at temperature 450˚C. Still, they reported that the valance band of the catalyst is remaining unchanged after treating with hydrogen, suggesting that the black color of the TiO_2 is entirely due to the point defect like oxygen vacancy (Diebold, 2004).

2.3 Nitrogen Doping TiO_2

In 2001, Asahi et al reported about the N-TiO2 where the band gap of the catalyst is founded to shift dramatically from the UV region to the visible light region from their absorption spectrum by sputtering TiO_2 into the N_2/Ar gas mixture. And it is also shown that due to this factor, the photo activity of the catalyst itself is also remarkably enhanced due to this factor. Since then, nitrogen doping has been receiving a lot of attention up until now. So far, several methods have been proposed around on the way to introduced nitrogen into TiO_2 such as:

1) Sol Gel Method (Livraghi et al, 2006), where the titanium dioxide pre-cursor is mix with N containing chemical to yield the TiO_2-N.

2) Reaction of TiO_2 with N-containing chemicals such as ammonia instead of nitrogen (Asahi et al, 2001).

3) Plasma Treatment Method (Chen et al, 2007), where the nitrogen is introduced into the TiO_2 by converting the nitrogen gas into plasma form.

4) Oxidizing the Ti-N film into TiO_2-N film (Zhu et al, 2010).

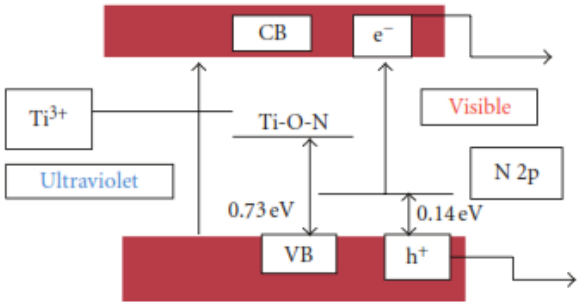

Figure 2.1: Formation of mid gap at forbidden band gap caused by Ti-O-N and chemisorb N in TiO_2 (Viswanathan et al, 2012).

Beside Asahi, several research groups (Irie et al, 2003; Sato, 1986; Beranek et al, 2007) also reporting that doping nitrogen into TiO_2 indeed has shifted the semiconductor from UV region to visible light region regardless of any method used to introduce N into the semiconductor, followed by the increasing of photo activity of the catalyst. As to explain the shift of absorption spectrum from UV region to visible region, Asahi et al proposed that the introduction of the mid gap caused by formation of Ti-O-N bond and the chemisorbed N_2 in the forbidden band gap. Another proposal has been suggested by Emeline et al (2007) where the reason for the visible light absorption is due to the formation of the oxygen vacancy and the Ti^{3+} in the TiO_2 lattice, while the function of N is to stabilize these defect only.

To proof the presence the existence of Ti-O-N bond and the chemisorbed N_2 in TiO_2 lattice, evidence is presented through the XPS analysis showing peaks at 396eV, 400eV and 402eV correspond to nitrogen N1s core level. It is proclaim that the N^-, or the Ti-O-N is being responsible for the peak 396eV while the chemisorbed N_2 is responsible to the peak 400eV and 402eV. These XPS analysis result also is supported by Viswanaten et al (2012), which had done a detailed review regarding the XPS results of N-TiO_2 catalyst collected from around the research group. According to Viswanaten et al (2012), although there is no consensus among the

results and researchers about the species assignment of the nitrogen 1s binding energy in N-TiO_2 catalyst up until now, still the group has concluded several rules of thumb that are helpful when analyzing the XPS results:

a) If N^- is present in the catalyst, then the valance state of Ti has to be different from Ti^{4+}.

b) N-1s-binding energy will normally appeared in the range 396-397eV when the nitrogen content in the system is very small. When the nitrogen content in the system is high, the higher binding energy (about 400eV) peak will appear also. This peak is considered as the chemisorbed nitrogen species on the catalyst surface in general.

c) The acceptable binding energy value of N 1s level in the substitute system is around 396-397eV. If the nitrogen is in anionic state, then the nitrogen-1s binding energy should be around 394eV. While if the nitrogen is in cationic state, the binding energy of the species should be around 400eV. Still this reading is unlikely to happen on the basis of the size and charge of the cation itself.

2.4 Hydrazine Wet Method

In 2007, Li et al has proposed a new way to synthesis the TiO_2-N using a very simple method, which is call the hydrazine method. In this method, the white powder TiO_2 is dipped in hydrazine hydrate (80%) for 12hr. The solution is then filtered and dried at 110˚C for 3 hours in air. The end product resulted a yellow color nitrogen doped TiO_2. Throughout this method, they successfully created a yellow N-TiO_2, where the light reflectance spectrum showing that the catalyst has shifted clearly from UV region to visible light region. The photoactivity test which is done via photocatalytic oxidation of ethylene into carbon dioxide also clearly indicates that the catalyst is able to boost the conversion of ethylene 0.5% to 9.5%.

During his experiment, Li et al (2007) realized that during the drying process, a glow is detected after evaporating a few solutions from the surface. Once the glow occurred, the catalyst is turned into yellow color. In 2012, Selvam et al also reported the same thing when they are using the exact same method to treat the TiO_2 pre-treated with combustion solution technique, where the glow is detected also during

the drying process and the catalyst becoming yellow after that. This lead the group to believe that during the drying process, combustion is occurred between hydrazine and the oxygen at 110 ˚C. In 2007, Rane et al has prepared their N-TiO_2 via sol gel method by utilizing hydrazine hydrate (99%) as the precursor. Here they mentioned that when the hydrazine exposed at lower temperature will reacts with the oxygen in the atmosphere as follows:

$$N_2H_4 + O_2 \rightarrow N_2 + 2H_2O \qquad \Delta H = -625 kJmol^{-1}$$

The glow that is detectable from eyesight can be due to the large amount of heat is liberated when the hydrazine is combusted. Rane et al (2007) also mentioned that in his reaction, the nitrogen that is formed by the combustion of hydrazine gets trapped in the lattice of TiO_2, yielding a yellow color nitrogen doped TiO_2. Hence from these 3 research group, we hypothesize that during the reaction, the hydrazine is combusted with the oxygen at 110˚C to give nitrogen and water. When the nitrogen is produced, the nitrogen will introduce into the TiO_2 with the help of enormous amount of heat that is released during the hydrazine combustion.

As to evidence that the nitrogen is successfully doped into the TiO_2 lattice, Li et al (2007) and Selvam et al (2012) has done XPS analysis on their samples. As for Li et al, a peak is found at 396.6eV from the XPS spectra for N1s core level. Li et al believe that this peak is correspond to Ti-N bond, which is the main reason on why the catalyst able to absorb the visible light. As for Selvam et al, a peak is found at 398.1eV from XPS spectra for N1s core level. Here they justify that this peak is assigned to anionic N in the Ti-O-N bond. Although both XPS analysis resulting different binding energy so far, still one thing can be confirm is that this combustion process is able to introduce nitrogen into TiO_2 lattice.

As to investigate whether this combustion will damage or alter the surface of the catalyst, the X-Ray Diffraction (XRD) analysis has been performed. From Li et al (2007) result, it can be seen that after the hydrazine combustion, the main peak of anatase phase at $2\theta=25.4^{\circ}$ is far sharper than the pretreated TiO_2. This shows that via the spontaneous combustion of hydrazine on the surface of TiO_2, the crystallization of TiO_2 has becoming better. Thus Li et al (2007) also proclaim them via this method; no further calcination is needed as the catalyst is already in the anatase

phase. While from Selvam et al (2012), the phase of TiO_2 after undergoing hydrazine treatment is in anatase since a significant sharp peak is shown at 25.43˚. Although the phase of the TiO_2 is already in anatase phase after the solution combustion technique, still one thing that can be proven here is that via this method, the phase of the TiO_2 will not be revert back from anatase to rutile phase. This is vital as it is evidence that the surface configuration of anatase phase TiO_2 can help in improving the photocatalytic activity of the catalyst itself (Diebold et al, 2004).

2.4.1 Interaction of Hydrazine with TiO_2

One thing worth mentioned here is the studies conducted by Chuang et al (2000) on the interaction of hydrazine on TiO_2 using Infra-Red (IR) spectroscopy studies. In this study, the TiO_2 is mounted inside the IR cell for FTIR spectrum analysis. Later on, N_2H_4 gas is introduced into the IR chamber at various temperatures. From the studies, it is found out that at 35˚C, an isolated hydroxyl group and several nitrogen species is bonded on TiO_2. When the temperature is increasing to 150˚C, the isolated hydroxyl group is decreasing along with the increment of temperature. But when the temperature is raised from 150˚C to 200˚C, the N_2H_4 adsorbed on the TiO_2 is further decompose to other N species or desorbed from the catalyst. At the same time the isolated hydroxyl adsorption in the range 3600-3800cm^{-1} is further enhanced along with this increment of temperature in this range. From here, a mechanism has been proposed to fit the result obtain from the FTIR as follows:

$$N_2H_4(ads) \rightarrow 2NH_2(ads) \rightarrow NH(ads) + NH_3(ads) \xrightarrow{O_{(lattice)}} OH(ads) + N(ads) + NH_3(ads)$$

Here the adsorbed N_2H_4 is decomposed to NH and NH_3 first. Then later on when the temperature is around 150˚C to 200˚C, the NH adsorbs will further decomposed to donate hydrogen atom to surface lattice oxygen atoms, generating OH and N adsorbed on the catalyst. One interesting fact to be found here is that the formation of the OH bond on the surface of the catalyst. As mentioned in previous section, one of the main factors that contribute to the band gap reduction is the formation of Ti-H bond that created the oxygen vacancy and the surface disorder as reported by Chen et

al (2011). Since there is no research reporting the catalyst with O-H bond, so it will be interesting to see the effect of this species on the photoactivity of the catalyst itself.

2.5 Methylene Blue Degradation Modeling

Here the reaction modeling of the methylene blue degradation modeling will be reviewed. The modeling is done as to characterize the reaction itself with an equation so that the reaction can be predictable under various operating condition. This modeling is important also as to provide the design equation to design the photocatalytic reactor, where the equation on the rate of reaction is needed in order to design the volume of the continuous reactor or the reaction time as for the batch reactor.

In 2013, a model has been proposed by Sannino et al (2013) to model a reaction considering the concentration of the methylene blue at that time, the intensity of the light and the weight of the catalyst used. Hence a methylene blue mass balance has been written as follows:

$$V \cdot \frac{dC(t)}{dt} = r(C, I) \cdot W_{\mathrm{TD}}$$

Here the V is the solution volume (L). C(t) is the methylene blue concentration (mgL^{-1}). *r* is the reaction rate ($gL^{-1}min^{-1}$). W_{TD} is the catalyst amount (g). And I is the light intensity reaching the catalyst surface ($mWcm^{-2}$).

Later on, the mass balance is further modelling the methylene blue concentration and the intensity of the light with the Langmuir-Hinshelwood mechanism rate law. Then, the Lambert-Beer law is used to further modelling the intensity of the light in the form Langmuir-Hinshelwood mechanism rate law again as to consider the screening effect, where the penetration of light decreases when the catalyst loading is increasing. Hence, the rate of degradation of methylene blue is written as follows:

$$V \cdot \frac{dC(t)}{dt} = -K_1 \cdot \frac{b \cdot C(t)}{1 + b \cdot C(t)} \cdot \frac{\alpha \cdot I_0 \cdot e^{-k_I \cdot [TiO_2]}}{1 + \alpha \cdot I_0 \cdot e^{-k_I \cdot [TiO_2]}} \cdot W_{TD}$$

Where:

K_1 = Kinetic constant (mg $g^{-1}min^{-1}$)

α = Light absorption coefficient ($cm^2(mW)^{-1}$)

k_1 = Specific extinction coefficient per unit catalyst mass (L mg^{-1})

I_0 = Light intensity incident on the reactor surface (mW cm^{-2})

$[TiO_2]$ = Catalyst dosage (mg L^{-1})

b = Adsorption coefficient (L mg^{-1})

Still several weaknesses have been detected within this model. As mentioned before, the intensity of the light here has been modelled referring to Langmuir-Hinshelwood mechanism rate law. As known, this Langmuir-Hinshelwood mechanism rate law is usually used to describe the reaction pathway of a catalytic reaction, where the reaction between two atoms is occurred when they are adsorbed on the surface of the catalyst as depicted as follows:

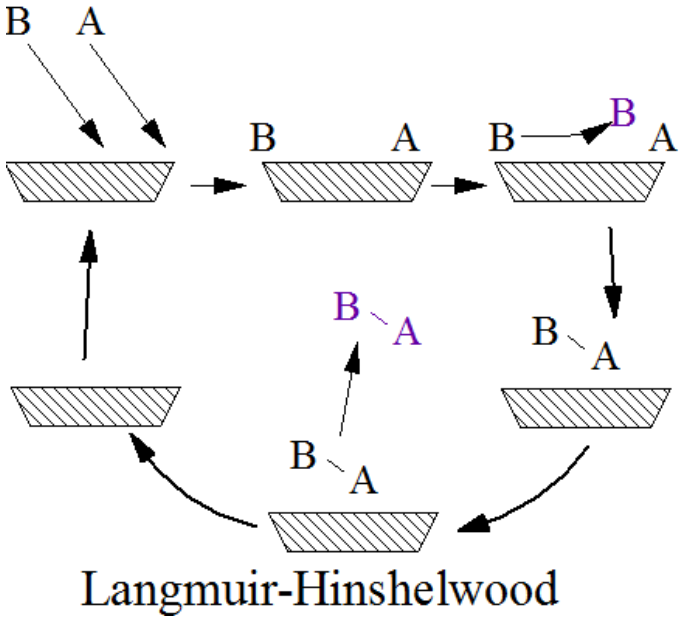

Figure 2.2: The reaction pathway of atoms as described by Langmuir-Hinshelwood mechanism rate law.

Hence, the doubt is raised when a rate law that characterize a reaction is used to model the effect of intensity of the light towards the degradation of the methylene blue itself. Concrete evidence showing the incompatibility of the light intensity model is shown when we recalculate back the constant considering the light intensity using the value provided by Sannio et al (2013) as shown below that is used to model their degradation for catalyst weight 0.3g and light intensity 32mWcm^{-1} in 100ml solution:

α = 0.000925 cm^2 (mW)$^{-1}$

I_0 = 32mWcm^{-1}

k_1 = 0.012Lmg^{-1}

[TiO_2] = catalyst weight/ solution volume = 0.3g/100ml = 3000mg/L

$$\frac{\alpha \times I_o \times e^{-k_1 \times [TiO_2]}}{1+\alpha \times I_o \times e^{-k_1 \times [TiO_2]}} = \frac{0.000925 \times 32 \times e^{-0.012 \times 3000}}{1+0.000925 \times 32 \times e^{-0.012 \times 3000}} = 6.87 \times 10^{-18} cm$$

This value suggested that after considering the light intensity factor for the degradation of methylene blue itself, the rate of degradation methylene blue is actually ranging around value of 10^{-18}cm, which is not in parallel with Sannio et al (2013) data. For the methylene blue degradation with 0.3g catalyst and light intensity 32mWcm^{-1}, the data of methylene blue concentration vs time is analysed and the graph of rate of methylene blue degradation vs concentration of methylene blue is generated using Origin software as shown in figure 2.3.

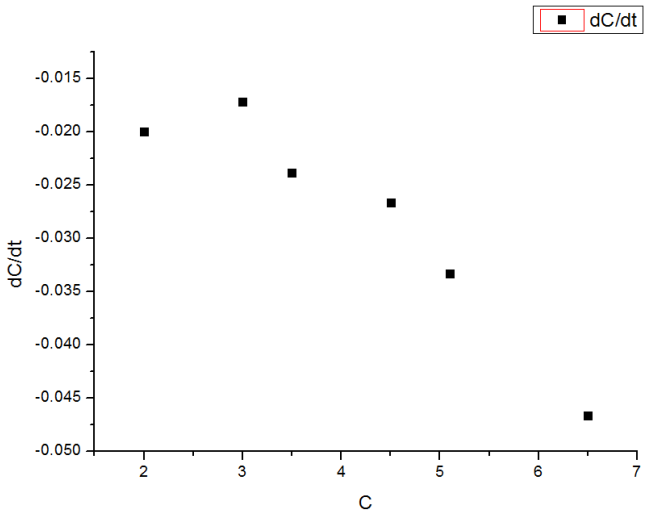

Figure 2.3: Graph of rate of methylene blue degradation vs concentration of methylene blue from Sannio et al (2013) data

As can be seen from the graph, the values of the rate of degradation are ranging around 0.075mgL^{-1}min^{-1} to 0.0475mgL^{-1}min^{-1}. Looking back at the model proposed, if we replacing the remaining available constant back in to model (K_1 = 0.46mg g^{-1} min^{-1}; b = 0.82L mg^{-1}; V = 100mL; W_{TD} = 0.3g; C_T = 2mg/L to 6.5mg/L), the rate of degradation obtained will be ranging around 10^{-18}, which is greatly deviating from the experimental data itself. Hence as for our experiment, another model of equation has been explored to characterize our degradation of our methylene blue which shown in chapter 4 later.

3 METHODOLOGY

3.1 Introduction

The experiment basically can be divided into 4 sections:

a) Catalyst Preparation

b) Photoactivity Test Measurement

c) Catalyst Characterization

d) Kinetic Study

3.1.1 Catalyst Preparation

In the photocatalyst preparation, the catalyst is prepared by referencing Li et al (2007) and Selvan et al (2012) preparation method, where the TiO_2 is basically immersed in the hydrazine for several hours, then dried in the oven at a 110˚C after being filtered. Based on this method, several modifications have been done to meet our objective of the research:

a) Ultra-sonication is done before and after mixing as to ensure that the catalyst is homogeneous in the hydrazine solution before drying.

b) The drying temperature is set at 60˚C and 170˚C referencing the temperature used by Li et al (2007) at 110˚C. This is done so as to study the effect of the temperature on the catalyst itself. This is done also as study the hypothesis where the combustion is happened on the surface of the catalyst in the dryer as mentioned by Kane et al (2007).

c) The powder is mortared after being dried in the oven. This is done as to grind the dried paste into powder form again. This is done also as to reduce the size of the powder as small as possible. Another reason for mortaring the powder is to observe the overall color of the powder itself.

3.1.2 Materials and Equipment

The materials that were used in the experiment are as followed:

1. Commercial TiO_2
2. Hydrazine Hydrate 64.5%

The commercial TiO_2 is provided by Shanghai Sunny Scientific Collaboration Co., Ltd from China. While the Hydrazine Hydrate 64.5% is purchased from Sigma Aldrich Company.

The equipment that was used in the experiment is:

1. Ventilated Oven
2. Ultra-sonication Bath
3. Mixing Plate
4. Filter Paper
5. Mortar

For the drying process, an oven is chosen to dry the catalyst instead of others oven available such as vacuum oven and heating plate since now it is desired also that the temperature of the oxygen is heated up to the specific reaction also so that the hypothesis made before can be accessed. While the ultra-sonication bath and the mixing plate chosen is of the common standard that is available around the lab. As for the filter paper, the filter paper is folded into fluted filter paper as to increase the rate of filtration of TiO_2 from hydrazine hydrate. The mortar used in the experiment is the marble mortar instead of the ceramic mortar as the mortar can be wash easily and to reduce the contamination of the catalyst as much as possible.

3.1.3 Procedure

The procedure for this experiment is described as followed:

1) 1g of commercial TiO_2 and 10ml of hydrazine hydrate (64.5%) is mixed in a beaker and covered with an aluminum foil.

2) The solution is ultra-sonic for 1 hour 30 minutes until the TiO_2 powder is homogeneous with the hydrazine hydrate in the beaker.

3) The aluminum foils is removed. And a magnetic stirred is inserted into the beaker.

4) The solution is stirred on the mixing plate for 12hr.

5) The solution is ultra-sonic again for 1 hour 30 minutes again.

6) The TiO_2 is filtered out from the solution using the fluted filter paper until 8ml of hydrazine hydrate is being filtered out from the solution.

7) The paste obtained from the filter paper is spread evenly on top of the petri dish.

8) The oven is preheated to 60˚C.

9) After reaching 60˚C, the petri dish is brought into the oven and dried for 3 hours. The color of the catalyst is observed for every 2 minutes until the changes in color on the catalyst are detected.

10) After 3 hours, the petri dish is removed out from the oven.

11) The dried paste in the petri dish is scratched out into a mortar. The paste is grinded into the powder for 5 minutes. The color of the powder is observed again after mortared.

3.2 Photoactivity Test Measurement

Photoactivity test are done as to evaluate the effectiveness of the catalyst to enhance the rate of reaction of the reactant in a reaction itself. In this study, this is usually done by performing the methylene blue degradation testing which is common around the paper (Sivalingam et al, 2003; Sanino et al, 2013). In the testing, the data on the methylene blue concentration along the reaction time is collected. Before the experiment start, a calibration curve is done as to relate the concentration of the methylene blue and the absorption height using UV-Vis spectrophotometer. This is done so that the concentration of methylene blue can be known via the UV-Vis spectrophotometer.

3.2.1 Materials and Equipment

The materials will be used in this part of experiment is as followed:

1. Methylene blue powder
2. Commercial TiO_2
3. TiO_2 treated at 170˚C

Here the stock solution of the 500ppm methylene blue is prepared from the powder provided. As to compare the rate of degradation of methylene blue using the catalyst before and after treated, the pure TiO_2 and TiO_2 dried at 170˚C is used in the experiment. The decision is made as from the experiment in previous section, it is found out that the catalyst treated at 170˚C has undergo much significant changes from the physical appearance as compared to the others as will be explain in Chapter 4 later.

The equipment used in this part of experiment is as followed:

1. Jacketed Batch Reactor
2. Water Cooling System
3. Black Box
4. Xenon Lamp
5. Mixing Plate
6. Centrifuge
7. HITACHI-U1800 UV-Vis Spectrophotometer

A small jacketed glass batch reactor is used in the reactor. The water cooling system is used to control the temperature of the reaction by circulating the water through the jacket of the reactor. The black box is used so that the reaction will not be affected by the surrounding light. The black box is used also so the dark reaction or catalyst adsorption can be performed before the photocatalytic reaction is started. To initiate the photocatalytic reaction, a xenon lamp is lighted on to propagate the high intensity visible light to the surface of the reaction. A mixing plate is used to ensure the photocatalyst is suspended in the aqueous solution. The centrifuge is used

to separate the methylene blue from the catalyst collected at a certain time so that the supernatant methylene blue can be collected. UV-Vis spectrophotometer is used to find the concentration of the methylene blue by calibrating the methylene blue concentration with the absorption height of the solution at a particular wavelength.

3.2.2 Procedure

For this experiment, the procedures can be further divided to few sections as follows:

1. Stock Solution Preparation
2. Calibration Curve
3. Photoactivity Reaction
4. Methylene Blue Concentration Measurement

3.2.2.1 Stock Solution Preparation

Here the preparation of 500ppm methylene blue stock solution is briefly described. To prepare the solution, 0.5g of methylene blue powder is mixed with 1L of deionized water in 1L volumetric flask. A well shake is given to ensure that the solution is well mixed.

3.2.2.2 Calibration Curve

Here the calibration curve between the concentration of methylene blue and the absorption height is plotted. The procedures are detailed as follows:

1) From the stock solution, the methylene blue with concentration 2ppm, 5ppm, 10ppm, and 15ppm are prepared from the stock solution.

2) The starting from 2ppm methylene blue, the solution is transferred into a cuvette.

3) The cuvette is inserted into UV-Vis spectrophotometer for analysis along with a blank solution.

4) After the result of the analysis obtained, the wavelength of the highest peak obtained and the absorption height for the peak are collected.

5) Repeat the steps above for 5ppm, 10ppm and 15ppm methylene blue solution again.

6) The graph of concentration of methylene blue and the absorption height is plotted using the data that is obtained from the above steps.

3.2.2.3 Photoactivity Reaction

In this section, we will be degrading 50ppm of methylene blue at 50ml with 0.1g of TiO_2 powder. Before the photocatalytic activity is started, the dark reaction is done to ensure that the degradation of the methylene blue measured is caused by reduction process that is induced by light instead of adsorption of the methylene blue on the catalyst.

The procedures for this part of experiment are as followed:

1) The setup for the black box, high intensity lamp, water cooling system, jacketed batch reactor and the mixing plate is done as shown in figure 3.1 and 3.2. The temperature of the water cooling system is set at 25˚C

2) 50ppm methylene blue in 50ml is prepared from the stock solution in a volumetric flask.

3) 0.01g of commercial TiO_2 is weighed and standby using the weighing machine.

4) The 0.01g TiO_2, 50ppm methylene blue and a medium sized magnetic stirrer is inserted into the batch reactor. In instant, the mixing plate is turned on to mixed the solution in dark condition for 2 hours.

Figure 3.1: Black Box

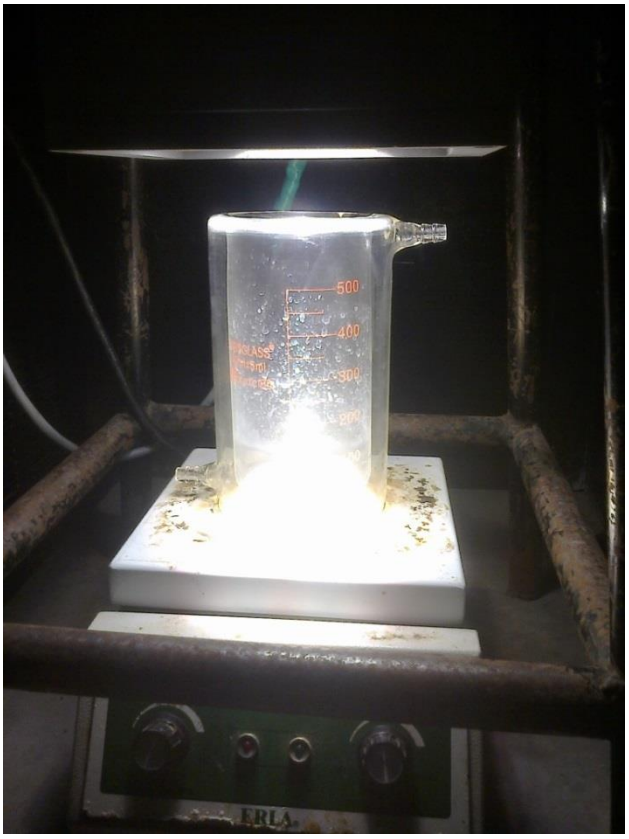

Figure 3.2: Set up of high intensity lamp, water cooling system, jacketed batch reactor and the mixing plate in the black box

5) After 2 hours, the mixing is stop. In instant, 1.5ml of solution is collected from the surface center of the solution itself using dropper and kept in a centrifuge tube. Then in a split second, the mixing is resumed again. At the same time the xenon light is switched on.

6) At 15 minutes starting from the previous step, the mixing is stop. In instant, 1.5ml of solution is collected from the surface center of the solution itself using dropper and kept in a centrifuge tube. Then in a split second, the mixing is resumed again.

7) Step 6 is repeated for every 15 minutes subsequently until for another 3 times. There will be 5 centrifuge tubes that are collected at the end of the experiment, where the tube is labeled as 0min, 15min, 30min, 45min and 60min respectively.

8) The experiment is repeated again using the 170˚C treated TiO_2.

In step 4, the stirring speed of the magnetic stirrer should not be vigorous to prevent to avoid the catalyst to splash around the side wall of the reactor. If this occurs, the amount of catalyst that is actually involved in the reaction is reduced, hence affecting the degradation of the methylene blue itself. In step 4 and step 5, the solution is taken from the surface center as to minimize the amount of catalyst to be taken away from the solution itself with the same reasoning as before.

3.2.2.4 Methylene Blue Concentration Measurement

Here, the concentration of the methylene blue is measured using the UV-Vis spectrophotometer and the calibration graphing that is prepared beforehand. The procedures for this part is as followed:

1) The solutions collected in the tubes from the previous experiment are centrifuged with rotational speed 5500rpm at 25˚C for 10 minutes.

2) Starting from 0min solution, the 1ml of supernatant liquid is collected from the tube itself and mixed with 9ml of deionized water in a volumetric flask.

3) The resultant mixture is transferred into a cuvette.

4) The cuvette is inserted into UV-Vis spectrophotometer for analysis along with the blank solution.

5) After the result of the analysis obtained, the wavelength of the highest peak obtained and the absorption height for the peak are collected.

6) Step 2 to 5 is repeated for the 15min, 30min, 45min and 60min solution.

7) Using the calibration curve, the graph of concentration versus time is plotted.

In step 4, the methylene blue is diluted with the dilution factors 10. The reason for this is that the effective height that the concentration of the methylene blue can be calibrated is ranging from 0.3 to 2.0 only. When the concentration of the methylene blue is too high, it will absorb all the light that is illuminated on it since the color of the methylene blue is too dark for the light to penetrate.

3.3 Catalyst Characterization

Catalyst characterization is done as to identify the some of the attributes of the catalyst itself. The properties among catalyst are then compared to evaluate the changes occurs in the catalyst itself. In this experiment, the properties that are interest thus far is the phase of the catalyst, the light absorption of the catalyst and the species adsorbed on the catalyst.

As to obtain the properties of the catalyst mentioned above, the analytical equipment is used to unveil those attribute through the data obtained from the machine itself. The phase of the catalyst is analyzed using Rigaku Miniflex X-Ray Diffractometer from Faculty of Science and Industry (FIST) in UMP. The X-Ray used in the machine is generated using CuKα radiation with wavelength 1.5418A. The Scherrer equation, $D = 0.89\lambda/\beta\cos\theta$ is employed to find the crystal size, where D is the crystal size, β is full width half maximum (FWHM), and θ is the diffraction angle. The optical properties of the catalyst are studied using the HR2000+ High-

resolution Spectrometer on the courtesy of Dr. Gurumurthy Hegde from FIST in UMP. While the FTIR spectra are done using Perkin Elmer Spectrum 100 model FTIR machine conducted in UKM on the courtesy of Mdm Hamidah Binti Abdullah from UKM.

3.4 Kinetic Studies

Reaction modeling is done as to characterize the reaction itself with an equation so that the reaction can be predictable under various operating condition. In the modeling, the software has been used for modeling are:

1) OriginPro 8

2) Microsoft Excel

Here the main function of the OriginPro 8 is to perform the differentiation function on the concentration of the methylene blue at specific time with respect to time. The numerical method that has been used to perform differentiation in the program is the high accuracy differentiation formula, where the first and the last value of the derivative are evaluated using the forward and backward finite-divided-difference formulas respectively. While the rest of the derivative is evaluated using the centered finite-divided-difference formula. The Microsoft Excel is used to fir the data obtain with the linear trend-line equation as to evaluate the constant for the proposed modeled equation as will be discussed in the next chapter.

4 RESULT AND DISCUSSION

4.1 Introduction

In this section, various data and results collected during experiment which has been pre-scribed in the previous chapter are analyzed and discussed. Here, we will be discussing on several items as followed:

1) UV-Vis Absorption Spectra analysis

2) XRD analysis

3) FTIR analysis

4) Methylene Blue Degradation

5) Kinetic study

4.2 UV-Vis Absorption Spectra Analysis

Here the color of the catalyst is discussed before moving on to the UV-Vis spectra of the catalyst. Figure 4.1 shows the color of the catalyst after the wet hydrazine treatment for commercial TiO2, 60˚C treated TiO_2 (N-TiO_2-60), 110˚C treated TiO_2 (N-TiO_2-110), and 170˚C treated TiO_2 (N-TiO_2-170). One fact about the color of the catalyst is that although the color change of the catalyst does not means that there is an element that is successfully doped into the catalyst, still the color change does indicate that some changes has happened on the catalyst.

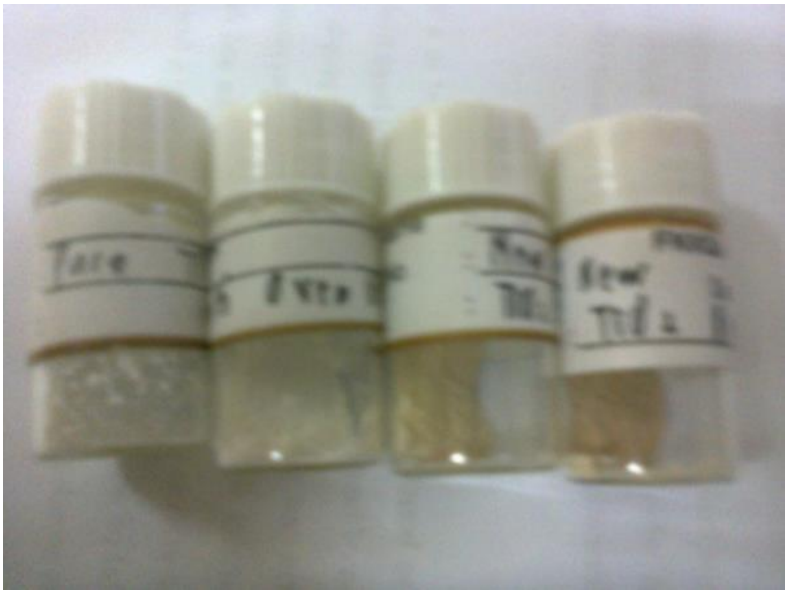

Figure 4.1: Color of the catalyst after the wet hydrazine treatment. From left: commercial TiO_2, N-TiO_2-60, N-TiO_2-110, and N-TiO_2-170.

In 2001, Asahi et al able to create the N-TiO_2 which is yellowish in color via sputtering TiO_2 in N_2(40%)/Ar gas mixture and annealed at 550˚C in N_2 gas for 4 hours. In 2010, Randorn et al successfully doped nitrogen into TiO_2 using free combustion method with TiN as the precursor. Rane et al (2007) able to create yellow color nitrogen doped TiO_2 via the prescribed novel hydrazine treatment. In 2007, Li et al are able to create a yellow N-TiO_2 catalyst using the wet hydrazine method. Using the same method, Selvam et al (2012) are able to create yellow N-TiO_2 catalyst also. From these journal, we can justified that when there is nitrogen species is involved in the catalyst preparation, then the changes in the color of the catalyst becoming yellow indicate that the nitrogen element is successfully doped into the lattice of the catalyst.

From our experiment, it can be seen that for the treated TiO_2 at 60˚C, the color of the catalyst still remain white. As for the TiO_2 treated at 110˚C, a light yellow yolk color TiO_2 is formed. And when the temperature is further raised to 170˚C, a dirty dark yellow yolk color TiO_2 is created. This finding proved the hypothesis that the combustion of hydrazine to doped the nitrogen into the TiO_2

lattice is shown. As the temperature of the oxygen is increase, the combustion is becoming more energetic, thus combust and trap the nitrogen into the TiO_2 lattice.

One interesting fact that is realized here is the dirty dark color imparted on the 170˚C treated TiO_2. In 2011, Chen et al reported a black color TiO_2 which is created due to the surface disordered formed on surface of the TiO_2 caused by the formation of Ti-H bond on the surface, which created the oxygen vacancy around the TiO_2 lattice. In 2000, when Chuang et al letting the hydrazine gas to react with TiO_2 at 150˚C to 200˚C, it is found out that isolated hydroxyl group is emerged and adsorbed on the surface of TiO_2, where the H group from the N_2H_4 is bonded to the lattice O in TiO_2. So here we hypothesis that there is a possibility that the formation of O-H bond has occurred in our catalyst as will be proven later via the FTIR analysis.

Figure 4.2 shows the absorbance spectra for the commercial TiO_2, N-TiO_2-60, N-TiO_2-110, and N-TiO_2-170. In this analysis, due to the unavailability of the quartz plate, we cannot observe the absorbance at the UV region, thus could not calculate the band gap of the semiconductor itself. This is because that during the sampling, the catalyst powder is dispersed on a glass plate to create the thin film. Since glass is opaque to ultraviolet light but transparent to the visible light, the absorbance reading at UV region is not available as the UV beam from the spectrophotometer is blocked by the glass itself. Nevertheless, the data available on the visible range will be good enough to proceed with our discussion as for now.

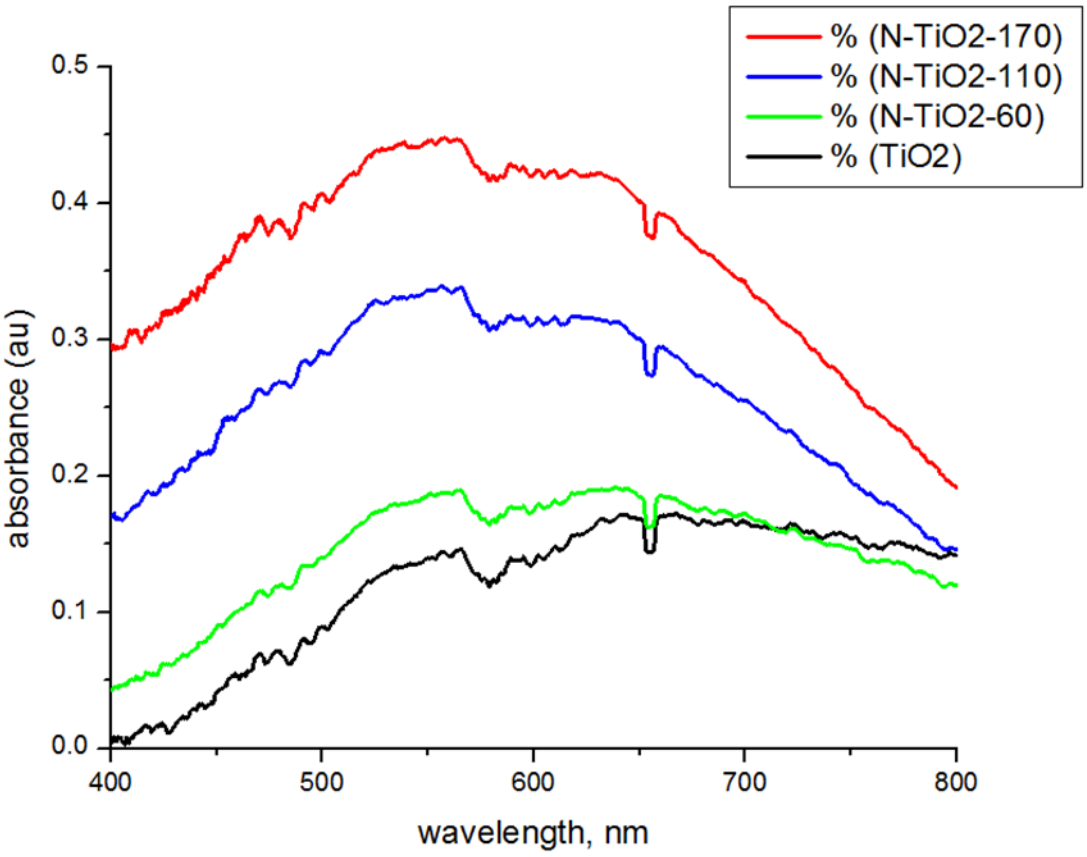

Figure 4.2: Absorbance spectra of the commercial TiO_2, N-TiO_2-60, N-TiO_2-110, and N-TiO_2-170.

From figure 4.2, it is obvious that at the visible light wavelength (400nm to 700nm), the 170˚C treated band gap is able to absorbed more visible light as compared to the commercial TiO_2. It is also noticed the visible absorption of the catalyst is increasing when the drying temperature is increasing also. Taking the basis of the change in color to intense yellow catalyst and the behavior of the UV-Vis spectra, we can infer that nitrogen element is doped into the TiO_2 lattice from the hydrazine hydrate, which created the mid-gap in the forbidden band gap that is responsible for the visible light absorption of the catalyst (Asahi et al, 2001). And as the temperature is increasing, more nitrogen is trapped into the TiO_2 lattice due to the more energetic combustion at higher temperature, causing the catalyst to be able to absorb more visible light as we have hypothesized in the 1st chapter.

From here, due to the time constrain and the financial issue that we faced in the project, we have screened the best catalyst available so far, N-TiO_2-170 to further our discussion.

4.3 FTIR Analysis

Here the FTIR spectra for the treated and the untreated TiO_2 are discussed. Figure 4.4 shows the FTIR spectra for the commercial TiO_2 and the N-TiO_2-170. From the figure, several peaks that relate to TiO_2 can be observed. The broad band centered at 500-600cm^{-1} is likely due to vibration of Ti-O bonds in TiO_2 lattice (Gao et al, 2003). While the peaks appeared at 1620-1630cm^{-1} and the broad peaks appearing at 3100-3600cm^{-1} are assigned to vibrations of hydroxyl groups (Klingenberg et al, 1996). As in the N-TiO_2-170, these peak that mentioned above overlap with the broad bands of the stretching and deformation modes of NH_x groups (Khabashesku et al, 2000). At the same time, a weak bond is appeared in the modified TiO_2 at 1200-1550cm^{-1} signifying the appearance of nitrogen oxide species (Navio et al, 1996). In the spectra for the 170˚C treated TiO_2, the sharp increase at the peak 1620-1630cm^{-1} and 3100-3600cm^{-1} also might be due to the increase of the isolated hydroxyl group as reported by Chung et al (2000) where the hydroxyl group is restored when the hydrazine gas is interacting with TiO_2 at temperature ranging from 150˚C to 200˚C.

Hence, from the FTIR spectra analysis, we can deduce that there are NH_x and few NO species that is appeared TiO_2 after hydrazine treatment. Another deduction can be made is that the increase in the OH functional group is observed after the hydrazine treatment.

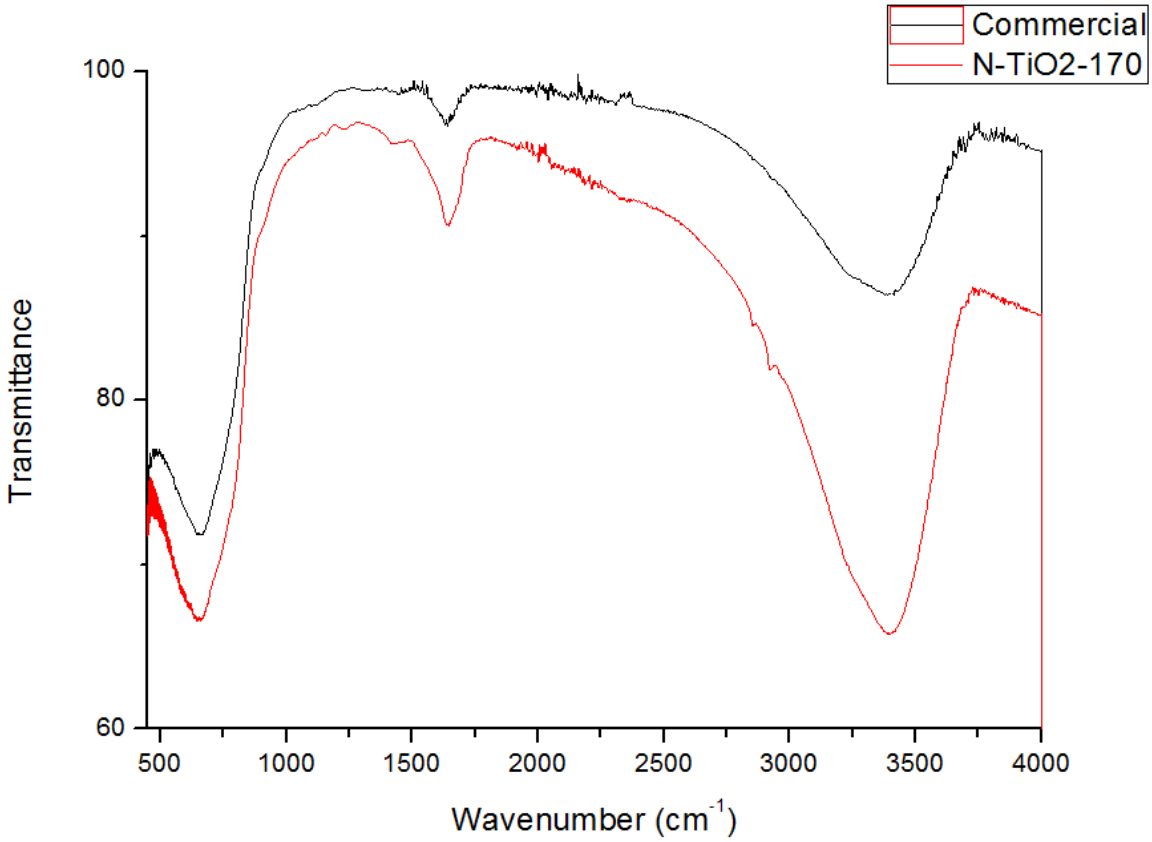

Figure 4.3: FTIR spectra for the commercial TiO_2 and N-TiO_2-170

4.4 XRD Analysis

Here we will be studying the phase of the catalyst via the XRD analysis. The X-Ray diffraction pattern for the commercial TiO_2 and the 170˚C treated TiO_2 are shown in the figure 4.2. From the figure, we can see that there is a main peak at 2θ = 25.32˚ which representing TiO_2 anatase phase. The peak observed at the specific 2θ which at 25.328˚, 37.76˚, 48.07˚, 53.93˚, 55.09˚, 62.83˚, 68.77˚, 70.25˚, and 75.01˚ is the diffraction of the crystal plane of anatase phase at (1,0,1), (1,0,3), (2,0,0), (1,0,5), (2,1,1), (2,1,3), (1,1,6) (2,2,0), and (2,1,5) respectively matching library available and provided by Rigaku XRD desktop. Hence we can confirm that both commercial TiO_2 and the 170˚C treated TiO_2 now is in anatase phase. This show that the method will not change the anatase phase back to the rutile phase again, as in accordance Selvam et al (2012) findings.

Besides the phase of the catalyst, we also studied the crystallinity of the catalyst. This is important as it is known that the crystallinity of the catalyst is beneficial to the photoactivity of the catalyst itself (Peng et al, 2005). To study the attribute, the intensity of both catalysts itself are evaluated. Observing the properties of the main peak of the anatase at 2θ=25.328˚ from figure 4.3, we can see that the intensity height of the catalyst is increasing from 647.95 to 671.59 after the commercial TiO_2 is treated at 170˚C. This increment shows that the crystallinity of the treated catalyst is slightly improved as compared to the commercial one. This founding is in parallel with Li et al (2003) XRD analysis result, where the intensity of the peak is increased significantly at anatase crystal plane after thy hydrazine wet treatment method.

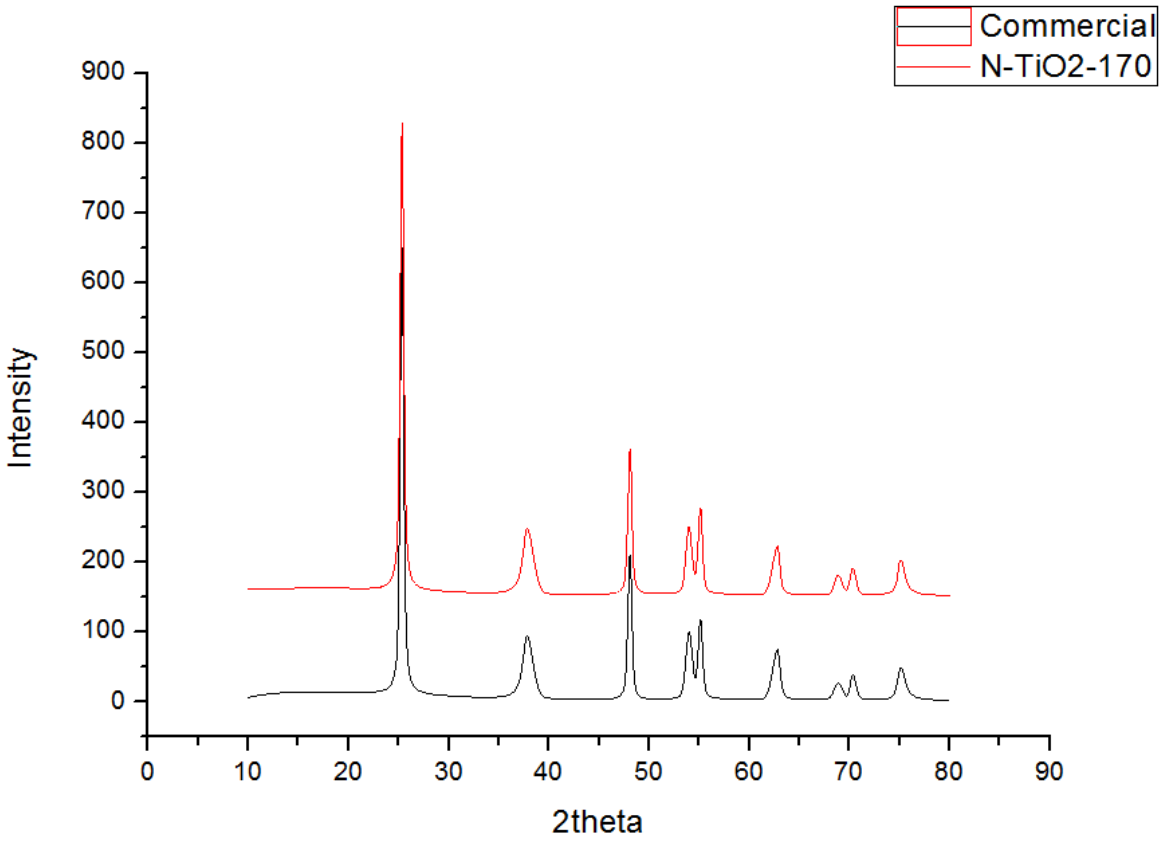

Figure 4.4: XRD Pattern for commercial TiO_2 and N-TiO_2-170

The size of the crystallite for both commercial TiO_2 and N-TiO_2-170 is also studied from the XRD pattern. Size of the crystal is important as the size will affect the band gap of the semiconductor directly also. As the size of crystal is small, the band gap of the semiconductor will be larger (Dong et al, 2007). The size of the crystal is calculated via the Scherer equation:

$$D = K\lambda/\beta \cos \theta$$

Here D is the size of the crystal. K is a constant with value 0.89 for TiO2 (Selvam et al, 2012). λ is the X-Ray wavelength which is 0.15418nm as default in Rigaku Miniflex X-Ray Diffractometer. B is the Full Width Half Maximum (FWHM) in radian available from the peak list in the appendix. And θ is the diffraction angle of the catalyst which is also available from the peak list in the appendix. The size of the crystal at 2θ=25.328˚ for both catalysts is calculated as follows:

$$D_{Tio2} = \frac{0.89 \times 0.15418}{0.00724 \times \cos(\frac{25.328}{2})} = 19.426nm$$

$$D_{N-Tio2-170} = \frac{0.89 \times 0.15418}{0.00719 \times \cos(\frac{25.328}{2})} = 19.561nm$$

From the calculation, the size of the crystal at 2θ= 25.328˚ for both commercial TiO_2 and N-TiO_2-170 is 19.426nm and 19.561nm respectively. This slight shift in the size of crystal is also evidence as modified catalyst can absorb visible light, signifying that the band gap of the crystal has been lowered due to the slight increase in the size of the crystal.

4.5 Methylene Blue Degradation

Here the photoactivity of the photocatalyst before and after the hydrazine treatment will be studied. The calibration curve between the absorbance height and the concentration of the methylene blue that will be used in this experiment is shown in figure 4.5, with the relation absorbance height (y) and the concentration of the methylene blue (x) is y = 0.1048x.

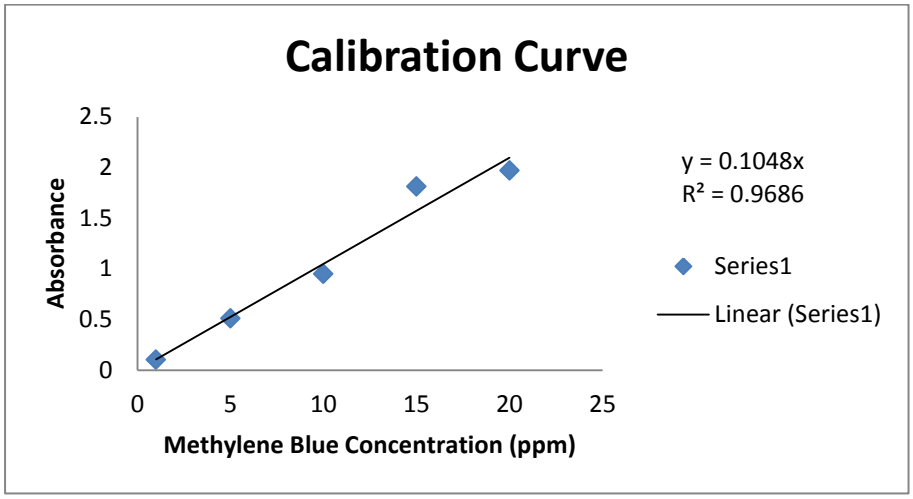

Figure 4.5: Calibration curve between concentration of the methylene blue and the absorbance height

Later on, the result of the absorbance of the solution from the reaction with commercial TiO_2 that were taken at specific time is measured as shown in Figure 4.6. Then later on the concentration of the methylene blue is calculated via the calibration curve as shown in table 4.1. The same process will be done for the reaction with 170˚C treated TiO_2 where the absorbance and the concentration of the methylene blue are shown in Figure 4.7 and table 4.2 respectively. Next, the photoactivity of both reactions after the dark reaction will be evaluated via C/C_0 graph as shown in figure 4.8.

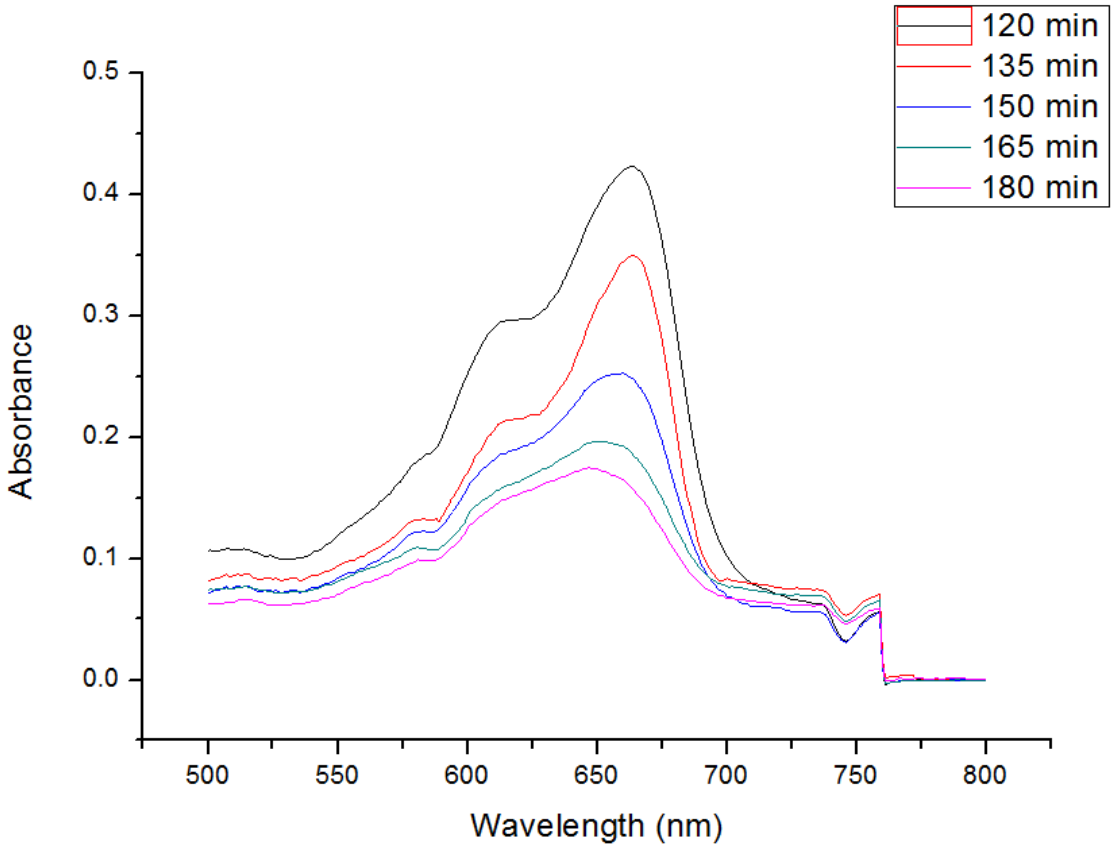

Figure 4.6: UV-Vis spectra for methylene blue collected from reaction with commercial TiO_2 at various time

Table 4.1: The concentration of the methylene blue (MB) along the reaction time from reaction with commercial TiO_2

Time	Absorbance (a.u)	MB Concentration (ppm)
0	0.524	49.9
120	0.410	39.05
135	0.351	33.43
150	0.265	25.24
165	0.211	20.10
180	0.190	18.10

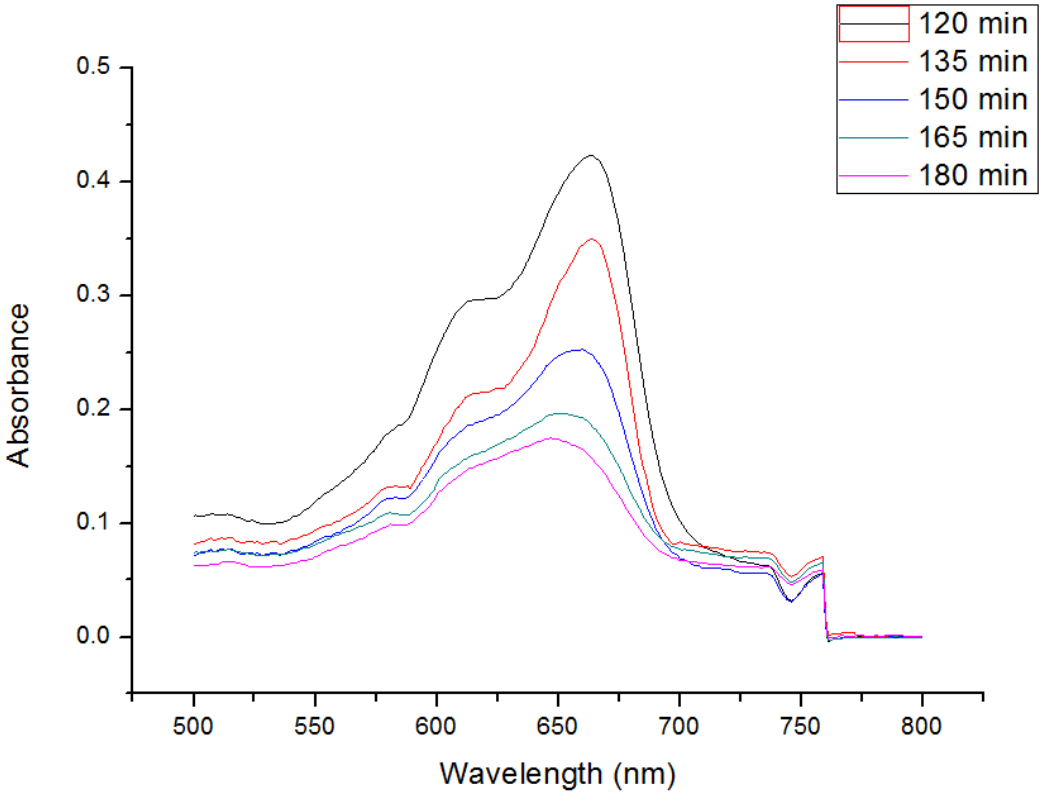

Figure 4.7: UV-Vis spectra for methylene blue collected from reaction with N-TiO_2-170 at various time

Table 4.2: The concentration of the methylene blue (MB) along the reaction time from reaction with N-TiO_2-170

Time	Absorbance (a.u)	MB Concentration (ppm)
0	0.524	49.90
120	0.401	38.19
135	0.320	30.48
150	0.245	23.33
165	0.189	18.00
180	0.154	14.67

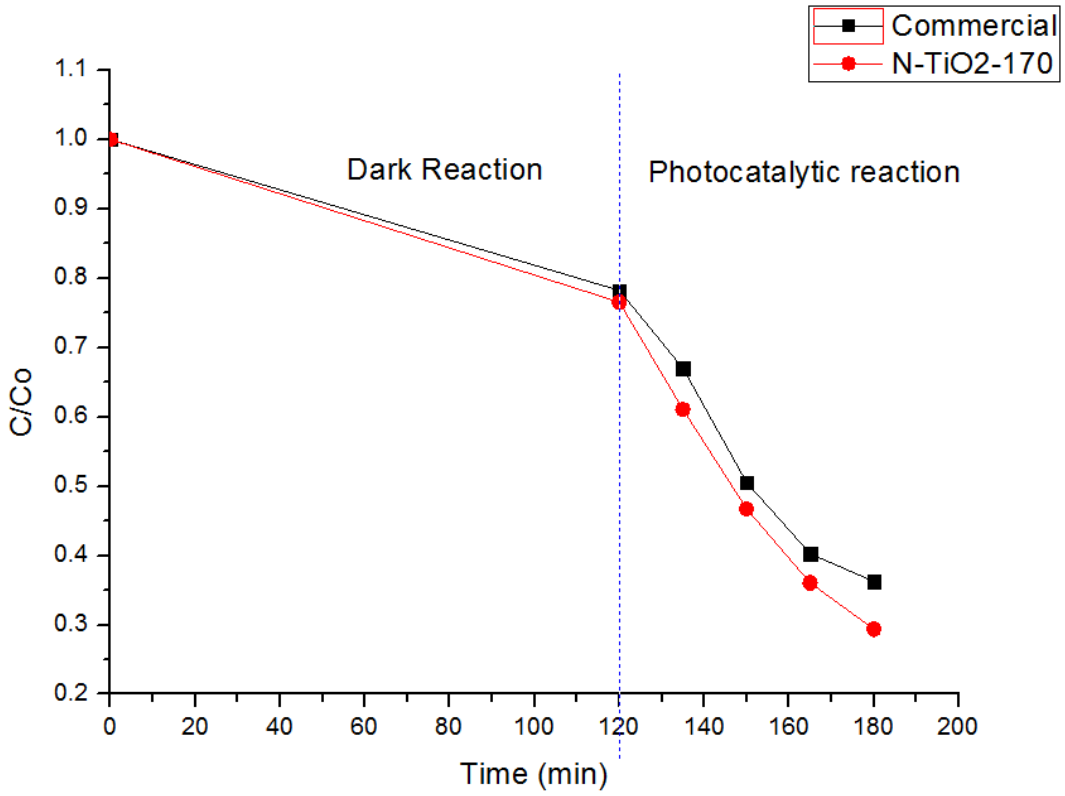

Figure 4.8: Degradation of methylene blue with commercial TiO_2 and N-TiO_2-170; Initial methylene blue concentration: 50ppm; Weight of catalyst: 0.01g

As from the table above, we can see there is not much change on the adsorption of the catalyst before and after the hydrazine treatment. Still this is not our main focus as we are more interested in the photoactivity of the catalyst now. When the light is turned on, we can see that there is a sharp decrease in the concentration of methylene blue, showing the significance of photo-reaction towards the degradation of methylene blue. Comparing both reactions, the methylene blue is degrading much faster when the 170˚C treated catalyst is used as compared to the commercial catalyst. Since so far the main difference between the commercial catalyst and the N-TiO_2-170 catalyst is that the treated catalyst can absorb more visible light as compare to the untreated one, we can deduced that this absorption of the visible light is responsible for the increase in photoactivity of the catalyst itself. When more light is being absorb into the catalyst, more electrons are excited from the valance band to the conduction band, thus producing more holes that is

responsible for the direct holes attack and the hydroxyl radical production as we are using the reaction pathway that is suggested by Sivalingam et al (2003).

4.6 Kinetic Studies

Here the reaction modeling is done for the reaction with N-TiO_2-170. The model that we used is the modeling considering the direct hole attack and the hydroxyl radical attack as proposed by Sivalingam et al (2003).

First the hole generation will be discussed. In the reaction, the hole is mainly generated from the excitation of electron from the valance band to conduction band, where the hole is left in the valance band after electron is excited as shown below:

$$TiO_2 + h\nu \xrightarrow{k_e} h_{VB}^{+} + e_{CB}^{-} \qquad \text{E.1}$$

The k_e is the reaction constant for this reaction.

At the same time, the holes produced will also undergo recombination of electrons again to generate the heat back as shown below:

$$h_{VB}^{+} + e_{CB}^{-} \xrightarrow{k_{rc}} \text{heat} \qquad \text{E.2}$$

The k_{rc} is the reaction constant for this reaction.

Later on, the hole generated will directly attack either the dye adsorbed on the surface of the catalyst, or the unbounded dye in the solution to yield the cationic dye radicals. And the radicals produced will further react to get the end species as shown below:

$$S - D + h_{VB}^{+} \xrightarrow{k_{hr}^{a}} S - D^{0+} \rightarrow \text{end species} \qquad \text{E.3}$$

$$D + h_{VB}^{+} \xrightarrow{k_{hr}^{b}} D^{0+} \rightarrow \text{end species} \qquad \text{E.4}$$

The k^{a}_{hr} and k^{b}_{hr} is the reaction constant for both reactions respectively; S-D is the dye adsorbed on the catalyst surface; D is the unbounded dye in the solution; and D^{0+} is the cationic radical dye generated by direct hole attack.

Next the hydroxyl radical generation will be discussed. The hydroxyl radical can be generated via the attack of hole on the hydroxyl group or the water adsorbed on the surface of the catalyst as shown below:

$$S - OH^{-} + h_{VB}{}^{+} \underset{k'_{tr}}{\overset{k_{tr}}{\rightleftharpoons}} S - \dot{O}H \qquad \text{E.5}$$

$$S - H_2O + h_{VB}{}^{+} \underset{k'_{tr}}{\overset{k_{tr}}{\rightleftharpoons}} S - \dot{O}H + H^{+} \qquad \text{E.6}$$

The k_{tr} and k'_{tr} is the reaction constant for the forward and backward reaction of both reversible reactions. S-OH^{-} is the anionic hydroxyl group that adsorbed on the catalyst surface. S-H_2O is the water group that is adsorbed on the catalyst surface. And S-OH· is the hydroxyl radical produced that is adsorbed on the surface.

Later, the adsorption and desorption of the mobile species in the reaction will be discussed. Here hydroxyl and dye can be adsorbed and desorbed away from surface of the catalyst as shown below:

$$S + D \underset{k'_D}{\overset{k_D}{\rightleftharpoons}} S - D, \quad K_D = \frac{k_D}{k'_D} \qquad \text{E.7}$$

$$S + \dot{O}H \underset{k'_{OH}}{\overset{k_{OH}}{\rightleftharpoons}} S - \dot{O}H, \quad K_{OH} = \frac{k_{OH}}{k'_{OH}} \qquad \text{E.8}$$

The k_D and k'_D is the reaction constant for the forward and backward reaction for E.8. And K_D is the equilibrium constant for the reaction E.7. While the k_{OH} and k'_{OH} is the reaction constant for the forward and backward reaction for E.8. And K_{OH} is the equilibrium constant for the reaction E.8

In the solution, since now both dye and hydroxyl radical is available either on catalyst surface or in the bulk, four possible combinations has been proposed where the reaction can occur: a) bounded hydroxyl radical and bounded dye; b) bounded hydroxyl radical and unbounded dye; c) unbounded hydroxyl radical and bounded dye; d) unbounded hydroxyl radical and unbounded dye as shown below:

Case (a):

$$S-D+S-\dot{O}H \xrightarrow{k_r^a} S+S-D'^{0}+M^{+}OH^{-} \qquad \text{E.9}$$

Case (b):

$$D+S-\dot{O}H \xrightarrow{k_r^b} S+D'^{0}+M^{+}OH^{-} \rightarrow \text{end species} \qquad \text{E.10}$$

Case (c):

$$S-D+\dot{O}H \xrightarrow{k_r^c} S-D'^{0}+M^{+}OH^{-} \rightarrow \text{end species} \qquad \text{E.11}$$

Case (d):

$$D+\dot{O}H \xrightarrow{k_r^a} D'^{0}+M^{+}OH^{-} \rightarrow \text{end species} \qquad \text{E.12}$$

The k_r^a, k_r^b, k_r^c, k_r^d is the reaction constant for each reactions respectively. D'^{0} is the cationic dye radical formed by hydroxyl radical attack. While the M^+ is the cation released from the dye molecule after being attack by hydroxyl radical.

Later on, relating the rate of disappearance of methylene blue to the direct hole attack mechanism (E.3 and E.4) and hydroxyl radical attack (E.9, E.10, E.11, E.12):

$$\begin{aligned} -r_D = {} & k_{hr}^a[S-D][h_{VB}^{+}] + k_{hr}^b[D][h_{VB}^{+}] \\ & + k_r^a[S-D][S-\dot{O}H] + k_r^b[D][S-\dot{O}H] \\ & + k_r^c[S-D][\dot{O}H] + k_r^d[D][\dot{O}H] \end{aligned} \qquad \text{E.13}$$

In order to define E.13 in a measurable parameter [D], several concentration formulas have been formulated out. From E.7 and E.8, the concentration of [S-D] and [S-ȮH] is further defined as follows:

$$[S-D] = K_D[S][D] \qquad \text{E.14}$$

$$[S-\dot{O}H] = K_{OH}[S][\dot{O}H] \qquad \text{E.15}$$

As to redefine [ȮH], a total hydroxyl radical balance has been done from E.5, E.6, E.9, E.10, E.11, and E.12 as follows:

$$\begin{aligned}&\frac{d([\dot{O}H]+[S-\dot{O}H])}{dt}\\ &= k_{tr}[S-OH^-][h_{VB}{}^+] - k'_{tr}[S-\dot{O}H]\\ &\quad + k_{tr}[S-H_2O][h_{VB}{}^+] - k'_{tr}[S-\dot{O}H][H^+]\\ &\quad - k_r^a[S-\dot{O}H][S-D] - k_r^b[S-\dot{O}H][D]\\ &\quad - k_r^c[\dot{O}H][S-D] - k_r^d[\dot{O}H][D]\end{aligned} \qquad \text{E.16}$$

It is well known that normally in a batch reaction, the reaction is normally pccured in unsteady state manner. Still as to ease our calculation at this stage, a quasi steady state assumption (QSSA) is made as to further evaluating E.16:

$$\frac{d([\dot{O}H]+[S-\dot{O}H])}{dt} = 0$$

$$[\dot{O}H] = \frac{k_{tr}\{[S-OH^-]+[S-H_2O]\}[h_{VB}{}^+]}{\begin{aligned}&K_{OH}\{k'_{tr}(1+[H^+])[S] + k_r^a[S-D][S]\\ &\quad + k_r^b[D][S]\} + k_r^c[S-D] + k_r^d[D]\end{aligned}} \qquad \text{E.17}$$

As to redefine [h^+_{VB}], a hole concentration balance is also done from E.1, E.2, E.5, and E.6 as follows:

$$\frac{d[h_{VB}{}^{+}]}{dt} = k_e[S] - k_{rc}[e_{CB}{}^{-}][h_{VB}{}^{+}] - k_{tr}[S-OH^{-}][h_{VB}{}^{+}] + k'_{tr}[S-\dot{O}H] - k_{tr}[S-H_2O][h_{VB}{}^{+}] + k'_{tr}[S-\dot{O}H][H^{+}] \quad \text{E.18}$$

Here, by assuming that the recombination process (E.2) is happening at faster rate as compared to other reaction and applying QSSA for E.18, E.18 can be further redefine to:

$$\frac{d[h_{VB}{}^{+}]}{dt} = 0$$

$$[h_{VB}{}^{+}] = \sqrt{\frac{k_e[S]}{k_{rc}}} \quad \text{E.19}$$

Substituting E.14, E.15, E.17 and E.19 back into E.13, we will be getting:

$$-\frac{d[D]}{dt} = k_{0h}[D] + \frac{k_0 K_0[D]}{1 + K_0[D]} \quad \text{E.20}$$

With the following constant that has been define along the substitution:

$$k_{0h} = k^{a}_{dch} + k^{b}_{dch}$$

$$k_0 = k_{dc} \quad \text{and} \quad K_0 = K^{a}_{DC} + K^{b}_{DC} + K^{c}_{DC} + K^{d}_{DC}$$

Parameters	Expressions
k^{a}_{dch}	$k^{a}_{hr} K_D[S] \sqrt{\frac{k_e[S]}{k_{rc}}}$
k^{a}_{dch}	$k^{b}_{hr} \sqrt{\frac{k_e[S]}{k_{rc}}}$
k_{dc}	$k_{tr}([S-OH^-] + [S-H_2O]) \sqrt{\frac{k_e[S]}{k_{rc}}}$
K^{a}_{DC}	$\frac{k^{a}_{r} K_D[S]}{k'_{tr}(1+[H^+])}$
K^{b}_{DC}	$\frac{k^{b}_{r}}{k'_{tr}(1+[H^+])}$
K^{c}_{DC}	$\frac{k^{c}_{r} K_D}{K_{OH} k'_{tr}(1+[H^+])}$
K^{d}_{DC}	$\frac{k^{d}_{r}}{K_{OH} k'_{tr}(1+[H^+])}$

The k_{0h} is the overall rate constant for direct hole attack, k_0 is the overall rate constant for hydroxyl radical attack. Both constant is dependent on the reaction conditions and the catalyst properties, but they are independent of the nature of the dye used. K_0 is the adsorption equilibrium constant dependent on the characteristic of dye and the rate –determining step.

In Sivalingam et al (2003) works, all the parameters are evaluated using the initial rate method so that the effect of the intermediates on the degradation can be neglected. Hence from E.20, their formula is further derived as followed:

$$\frac{1}{r_{D0}} = \frac{1}{K_0((k_{0h}/K_0) + k_0)} \frac{1}{[D]_0} + \frac{1}{(k_{0h}/K_0) + k_0}$$

Still, instead of evaluating at the initial rate method and neglecting the effect of the intermediate towards the reaction, we will fit the model with the data obtain along the time reaction as we believe that those effect are important also to be considered and to be characterized into the model as what has been done by Sanino et al (2013). Hence, after reshuffling E.20, we are getting:

$$\frac{-1}{r_{Dt}} = \frac{1}{K_0(\frac{k_0 h}{K_0}+k_0)}\frac{1}{[D]_t} + \frac{1}{\frac{k_0 h}{K_0}+k_0}$$

Here r_{Dt} is the rate of degradation of the methylene blue at specific time. And $[D]_t$ is the concentration of the methylene blue at the specific time.

From table 4.2, the data of methylene blue concentration is differentiated with respect to time to obtain the rate of degradation of methylene blue as shown in figure 4.9. Later on, a plot of -1/rate of methylene blue degradation at specific time versus the concentration of the methylene blue at the same time will be plotted as shown in figure 4.10. A trend-line is included as the result of fitting the plotted line to the linear equation.

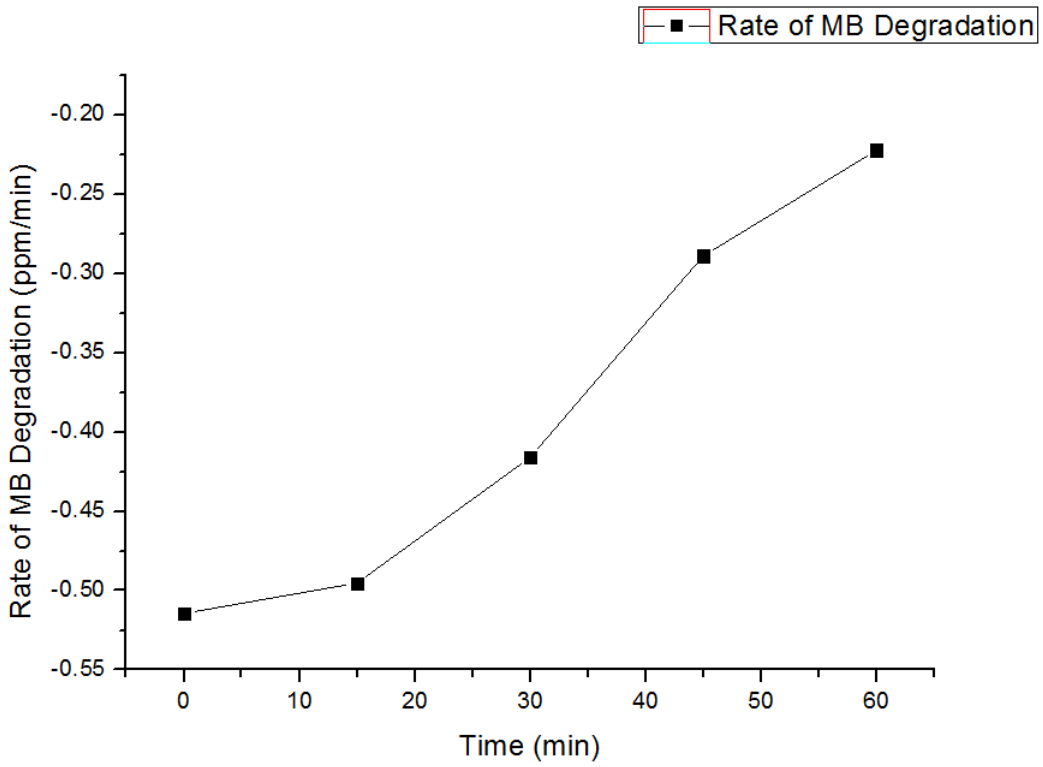

Figure 4.9: Graph of rate of methylene blue (MB) degradation over time

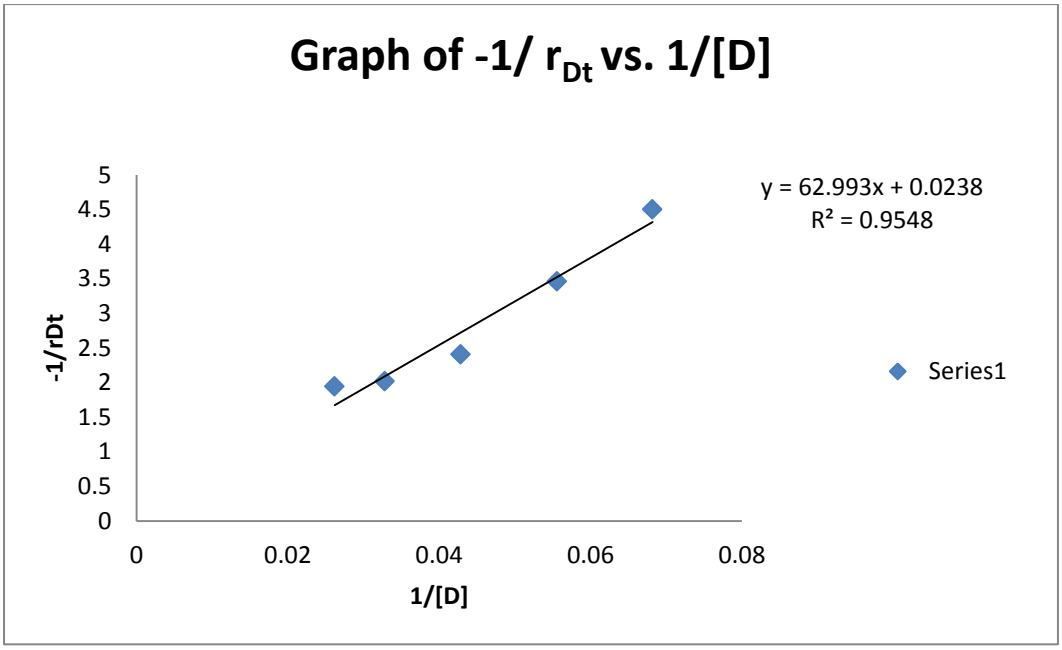

Figure 4.10: Graph of -1/rate of methylene blue degradation versus the 1/concentration of the methylene blue

From figure 4.10, the fitted linear equation obtained is y=51.309x + 0.3876. This fitted equation is acceptable as the R^2 obtained as a result of fitting is above 0.95. Hence, comparing the model equation and the fitted linear equation from figure 4.10, we obtained (k_{0h}/K_0+k_0) = 42.012 mg L^{-1} min^{-1}, while $K_0=3.78x10^{-4}$L mg^{-1}. According to Sivalingam et al (2003), the higher value of K_0 implies the blocking of the active sites of the catalyst due to strong adsorption, while the higher value of (k_{0h}/K_0+k_0) indicating the higher degradation rates of the dye.

5 CONCLUSION AND RECOMMENDATION

5.1 Conclusion

Here the conclusion is done to review back what are outlined in the report. In chapter 1, the objectives of the project are:

1) To synthesis N-TiO_2 that absorbs light in visible region using wet hydrazine method.

2) To inspect the photoactivity of the modified TiO2.

3) To model the methylene blue degradation reaction.

Two hypotheses are made in this chapter regarding the reactions that are occurred during the hydrazine wet method, where we speculate combustion and the decomposition of N_2H_4(ads) to OH(ads) are occurring during the reaction. We expected that from the project, we will see that the nitrogen is successfully doped inside the TiO_2 lattice via hydrazine combustion. We are also expecting that the photocatalytic activity of the N-TiO_2 is increased compared to the commercial TiO_2 due to the increase of the visible light absorption of the N-TiO_2, and the modeling on the methylene blue degradation with the modified catalyst is done when the project is ended.

In chapter 2, the literature review has been done focusing on the general strategies that is implemented in the academic in recent years to bring the light absorption of the TiO_2 from the ultraviolet range to the visible range. Strategies that is reviewed including creation of Ti^{3+} defect site, oxygen vacancy, surface disordered layer, and nitrogen doping. Next the literature review is also done on the relation to be used in the modeling of the methylene blue degradation.

In chapter 3, the methodology of the project is detailed in this chapter. The experiment can be divided into 2 parts: catalyst preparation and the photoactivity test

measurement. The modification that is done referencing the Li et al (2007) and Selvam et al (2012) work is also listed out. For each part of experiment, the materials, equipment needed and procedure of the experiment is stated. As for the modeling, the software to be used and their purposed are also listed in this chapter too.

In chapter 4, the result obtained from the experiment is analyzed and discussed. From the UV/Visible absorption spectra, we founded that the modified TiO_2 can absorb more visible light as compared to the commercial TiO_2. We also realized that as drying temperature increases, the color of TiO_2 is changing from white to intense yellow, making us believe that the main reaction occurred in the modification is indeed combustion of hydrazine on the surface of TiO_2, From the XRD spectra, we noticed that the phase of both commercial and the 170˚C treated TiO_2 is anatase phase. We also noticed that the modified catalyst is more crystalline compared to the commercial TiO_2. From the FTIR spectra, we infer that NH_x group, NO group is presented in TiO_2 after the treatment. At the same time, amount of OH group that is presented in TiO_2 is increased after the treatment. From the methylene blue degradation, the photoactivity of the after modified TiO_2 is higher than the commercial TiO_2. With all the founding above, we deduced that the increase the photoactivity is due to the improvement of the visible light absorption after the modification, hence achieving the 1st and 2nd objectives. As for the modeling, the equation to be used to characterize the methylene blue degradation is as followed:

$$\frac{1}{r_{Dt}} = \frac{-1}{K_0\left(\frac{k_{0h}}{K_0}+k_0\right)}\frac{1}{[D]_t} + \frac{1}{\frac{k_{0h}}{K_0}+k_0}$$

After the line fitting is performed, the value of the constant obtained are (k_{0h}/K_0+k_0) = 2.5799ppm min^{-1}, while $K_0=7.55x10^{-3}ppm^{-1}$, thus accomplished our 3rd objective.

5.2 Recommendation

In order to study the changes in band gap before and after the modification, the UV-Vis spectrum at the UV range and the visible range is needed. Hence, the UV-Vis spectrum analysis should be done via the spectrophotometer that is capable

to analyze the powder sample such as the PerkinElmer Lambda 35 UV/Vis Spectrophotometer and the Shimadzu UV 2450 model UV/Vis Spectrophotometer.

As mentioned, the FTIR spectrum to an extent is able to infer the presence of the species in the catalyst only. As to have a concrete evidence of the species presented in the lattice of the TiO_2, X-ray Photoelectron Spectroscopy studies should be performed as to identify the electronic state of the species presented in the lattice of the TiO_2. Via XPS studies, the molecule bonding that is responsible for surface defect which reduce the band gap could be identified also.

REFERENCES

Asahi, R., Morikawa, T., Ohwaki, T., Aoki, K., & Taga, Y. (2001). Visible-Light Photocatalysis in Nitrogen-Doped Titanium Oxides. *Science, 293*(5528), 269-271. doi: 10.1126/science.1061051

Beranek, R., & Kisch, H. (2008). Tuning the optical and photoelectrochemical properties of surface-modified TiO2. [10.1039/B711658F]. *Photochemical & Photobiological Sciences, 7*(1), 40-48. doi: 10.1039/b711658f

Bulut, Y., & Aydın, H. (2006). A kinetics and thermodynamics study of methylene blue adsorption on wheat shells. *Desalination, 194*(1–3), 259-267. doi: http://dx.doi.org/10.1016/j.desal.2005.10.032

Chen, C., Bai, H., Chang, S.-m., Chang, C., & Den, W. (2007). Preparation of N-doped TiO2 photocatalyst by atmospheric pressure plasma process for VOCs decomposition under UV and visible light sources. *Journal of Nanoparticle Research, 9*(3), 365-375. doi: 10.1007/s11051-006-9141-2

Chen, X., Liu, L., Yu, P. Y., & Mao, S. S. (2011). Increasing Solar Absorption for Photocatalysis with Black Hydrogenated Titanium Dioxide Nanocrystals. *Science, 331*(6018), 746-750. doi: 10.1126/science.1200448

Chuang, C.-C., Shiu, J.-S., & Lin, J.-L. (2000). Interaction of hydrazine and ammonia with TiO2. [10.1039/B001389G]. *Physical Chemistry Chemical Physics, 2*(11), 2629-2633. doi: 10.1039/b001389g

Cronemeyer, D. C. (1959). Infrared Absorption of Reduced Rutile TiO_{2} Single Crystals. *Physical Review, 113*(5), 1222-1226.

Diebold, U. (2003). The surface science of titanium dioxide. *Surface Science Reports, 48*(5–8), 53-229. doi: http://dx.doi.org/10.1016/S0167-5729(02)00100-0

Emeline, A. V., Sheremetyeva, N. V., Khomchenko, N. V., Ryabchuk, V. K., & Serpone, N. (2007). Photoinduced Formation of Defects and Nitrogen Stabilization of Color Centers in N-Doped Titanium Dioxide. *The Journal of Physical Chemistry C, 111*(30), 11456-11462. doi: 10.1021/jp071181v

Fu, Q. (2003). Radiation (SOLAR). In R. H. Editor-in-Chief: James (Ed.), *Encyclopedia of Atmospheric Sciences* (pp. 1859-1863). Oxford: Academic Press.

Gao, Y., Masuda, Y., Peng, Z., Yonezawa, T., & Koumoto, K. (2003). Room temperature deposition of a TiO2 thin film from aqueous peroxotitanate solution. [10.1039/B208681F]. *Journal of Materials Chemistry, 13*(3), 608-613. doi: 10.1039/b208681f

Irie, H., Washizuka, S., Yoshino, N., & Hashimoto, K. (2003). Visible-light induced hydrophilicity on nitrogen-substituted titanium dioxide films. [10.1039/B302975A]. *Chemical Communications, 0*(11), 1298-1299. doi: 10.1039/b302975a

Jiang, Z., Xiao, T., Kuznetsov, V. L., & Edwards, P. P. (2010). Turning carbon dioxide into fuel. *Philosophical Transactions of the Royal Society A: Mathematical, Physical and Engineering Sciences, 368*(1923), 3343-3364. doi: 10.1098/rsta.2010.0119

Khabashesku, V. N., Zimmerman, J. L., & Margrave, J. L. (2000). Powder Synthesis and Characterization of Amorphous Carbon Nitride. *Chemistry of Materials, 12*(11), 3264-3270. doi: 10.1021/cm000328r

Kim, D. S., & Kwak, S.-Y. (2007). The hydrothermal synthesis of mesoporous TiO2 with high crystallinity, thermal stability, large surface area, and enhanced photocatalytic activity. *Applied Catalysis A: General, 323*(0), 110-118. doi: http://dx.doi.org/10.1016/j.apcata.2007.02.010

Klingenberg, B., & Vannice, M. A. (1996). Influence of Pretreatment on Lanthanum Nitrate, Carbonate, and Oxide Powders. *Chemistry of Materials, 8*(12), 2755-2768. doi: 10.1021/cm9602555

Li, D., Huang, H., Chen, X., Chen, Z., Li, W., Ye, D., & Fu, X. (2007). New synthesis of excellent visible-light TiO2−xNx photocatalyst using a very simple method. *Journal of Solid State Chemistry, 180*(9), 2630-2634. doi: http://dx.doi.org/10.1016/j.jssc.2007.07.009

Linsebigler, A. L., Lu, G., & Yates, J. T. (1995). Photocatalysis on TiO2 Surfaces: Principles, Mechanisms, and Selected Results. *Chemical Reviews, 95*(3), 735-758. doi: 10.1021/cr00035a013

Liu, L., Zhao, H., Andino, J. M., & Li, Y. (2012). Photocatalytic CO2 Reduction with H2O on TiO2 Nanocrystals: Comparison of Anatase, Rutile, and Brookite Polymorphs and Exploration of Surface Chemistry. *ACS Catalysis, 2*(8), 1817-1828. doi: 10.1021/cs300273q

Livraghi, S., Paganini, M. C., Giamello, E., Selloni, A., Di Valentin, C., & Pacchioni, G. (2006). Origin of Photoactivity of Nitrogen-Doped Titanium Dioxide under Visible Light. *Journal of the American Chemical Society, 128*(49), 15666-15671. doi: 10.1021/ja064164c

Lu, G., Linsebigler, A., & Yates, J. T. (1994). Ti3+ Defect Sites on TiO2(110): Production and Chemical Detection of Active Sites. *The Journal of Physical Chemistry, 98*(45), 11733-11738. doi: 10.1021/j100096a017

Naldoni, A., Allieta, M., Santangelo, S., Marelli, M., Fabbri, F., Cappelli, S., . . . Dal Santo, V. (2012). Effect of Nature and Location of Defects on Bandgap Narrowing in Black TiO2 Nanoparticles. *Journal of the American Chemical Society, 134*(18), 7600-7603. doi: 10.1021/ja3012676

Navio, J. A., Cerrillos, C., & Real, C. (1996). Photo-induced Transformation, upon UV Illumination in Air, of Hyponitrite SpeciesN2O22- Preadsorbed onTiO2 Surface. *Surface and Interface Analysis, 24*(5), 355-359. doi: 10.1002/(sici)1096-9918(199605)24:5<355::aid-sia122>3.0.co;2-d

Peng, T., Zhao, D., Dai, K., Shi, W., & Hirao, K. (2005). Synthesis of Titanium Dioxide Nanoparticles with Mesoporous Anatase Wall and High Photocatalytic Activity. *The Journal of Physical Chemistry B, 109*(11), 4947-4952. doi: 10.1021/jp044771r

Randorn, C., & Irvine, J. T. S. (2010). Synthesis and visible light photoactivity of a high temperature stable yellow TiO2 photocatalyst. [10.1039/C0JM01370F]. *Journal of Materials Chemistry, 20*(39), 8700-8704. doi: 10.1039/c0jm01370f

Rane, K. S., Uskaikar, H., Pednekar, R., & Mhalsikar, R. (2007). The low temperature synthesis of metal oxides by novel hydrazine method. *Journal of Thermal Analysis and Calorimetry, 90*(3), 627-638. doi: 10.1007/s10973-007-8515-8

Sannino, D., Vaiano, V., Sacco, O., & Ciambelli, P. (2013). Mathematical modelling of photocatalytic degradation of methylene blue under visible light irradiation. *Journal of Environmental Chemical Engineering, 1*(1–2), 56-60. doi: http://dx.doi.org/10.1016/j.jece.2013.03.003

Sato, S. (1986). Photocatalytic activity of NOx-doped TiO2 in the visible light region. *Chemical Physics Letters, 123*(1–2), 126-128. doi: http://dx.doi.org/10.1016/0009-2614(86)87026-9

Selvam, K., & Swaminathan, M. (2012). Nano N-TiO2 mediated selective photocatalytic synthesis of quinaldines from nitrobenzenes. [10.1039/C2RA01178F]. *RSC Advances, 2*(7), 2848-2855. doi: 10.1039/c2ra01178f

Sivalingam, G., Nagaveni, K., Hegde, M. S., & Madras, G. (2003). Photocatalytic degradation of various dyes by combustion synthesized nano anatase TiO2. *Applied Catalysis B: Environmental, 45*(1), 23-38. doi: http://dx.doi.org/10.1016/S0926-3373(03)00124-3

Viswanathan, B., & Krishanmurthy, K. R. (2012). Nitrogen Incorporation in TiO2: Does It Make a Visible Light Photo-Active Material? *International Journal of Photoenergy, 2012*, 10. doi: 10.1155/2012/269654

Wang, G., Wang, H., Ling, Y., Tang, Y., Yang, X., Fitzmorris, R. C., . . . Li, Y. (2011). Hydrogen-Treated TiO2 Nanowire Arrays for Photoelectrochemical Water Splitting. *Nano Letters, 11*(7), 3026-3033. doi: 10.1021/nl201766h

Wei, W., Yaru, N., Chunhua, L., & Zhongzi, X. (2012). Hydrogenation of TiO2 nanosheets with exposed {001} facets for enhanced photocatalytc activity. [10.1039/C2RA21049E]. *RSC Advances, 2*(22), 8286-8288. doi: 10.1039/c2ra21049e

Xiong, L.-B., Li, J.-L., Yang, B., & Yu, Y. (2012). Ti3+ in the Surface of Titanium Dioxide: Generation, Properties and Photocatalytic Application. *Journal of Nanomaterials, 2012*. doi: 10.1155/2012/831524

Zhu, L., Xie, J., Cui, X., Shen, J., Yang, X., & Zhang, Z. (2010). Photoelectrochemical and optical properties of N-doped TiO2 thin films prepared by oxidation of sputtered TiNx films. *Vacuum, 84*(6), 797-802. doi: http://dx.doi.org/10.1016/j.vacuum.2009.10.040

Zollinger, H. (1992). Color Chemistry as Reflected in Helvetica Chimica Acta. *Helvetica Chimica Acta, 75*(6), 1727-1754. doi: 10.1002/hlca.19920750602

Zuo, F., Wang, L., Wu, T., Zhang, Z., Borchardt, D., & Feng, P. (2010). Self-Doped Ti3+ Enhanced Photocatalyst for Hydrogen Production under Visible Light.

Journal of the American Chemical Society, 132(34), 11856-11857. doi: 10.1021/ja103843d

APPENDICES

Table A.1: Peak List for the commercial TiO_2 from XRD analysis

Peak list

2-theta (deg)	d (ang.)	Height (cps)	Int. I(cps¥deg)	FWHM(deg)	Phase name
25.318(8)	3.5150(11)	435(21)	250(2)	0.415(7)	Anatase, syn, (1,0,1)
37.77(3)	2.3800(16)	60(8)	93.6(19)	1.19(3)	Anatase, syn, (1,0,3)
48.034(18)	1.8925(7)	147(12)	87.7(14)	0.452(14)	Anatase, syn, (2,0,0)
53.96(3)	1.6979(8)	65(8)	58.3(15)	0.74(3)	Anatase, syn, (1,0,5)
55.08(2)	1.6660(7)	78(9)	46.6(14)	0.49(2)	Anatase, syn, (2,1,1)
62.83(4)	1.4778(9)	49(7)	49.2(11)	0.84(4)	Anatase, syn, (2,1,3)
68.77(6)	1.3639(11)	16(4)	16.1(7)	0.96(6)	Anatase, syn, (1,1,6)
70.22(4)	1.3392(7)	25(5)	17.1(8)	0.65(3)	Anatase, syn, (2,2,0)
75.08(3)	1.2642(5)	32(6)	39.5(12)	0.86(4)	Anatase, syn, (2,1,5)

Table A.2: Peak List for the N-TiO_2-170 from XRD analysis

Peak list

2-theta (deg)	d (ang.)	Height (cps)	Int. I(cps¥deg)	FWHM(deg)	Phase name
25.326(8)	3.5139(11)	455(21)	262(2)	0.412(7)	Anatase, syn, (1,0,1)
37.76(2)	2.3805(14)	63(8)	95.9(18)	1.21(3)	Anatase, syn, (1,0,3)
48.07(2)	1.8910(7)	147(12)	86.1(14)	0.437(15)	Anatase, syn, (2,0,0)
53.93(3)	1.6988(9)	65(8)	54.7(16)	0.69(3)	Anatase, syn, (1,0,5)
55.09(2)	1.6658(7)	85(9)	49.1(15)	0.48(2)	Anatase, syn, (2,1,1)
62.83(2)	1.4777(4)	48(7)	46.3(12)	0.82(2)	Anatase, syn, (2,1,3)
68.77(5)	1.3639(9)	19(4)	17.1(7)	0.86(5)	Anatase, syn, (1,1,6)
70.25(4)	1.3388(7)	26(5)	18.0(8)	0.65(3)	Anatase, syn, (2,2,0)
75.01(2)	1.2652(4)	37(6)	42.7(12)	0.74(3)	Anatase, syn, (2,1,5)

TECHINCAL PAPER

MODIFICATION OF TITANIUM DIOXIDE NANOPARTICLE TO ENHANCE THE PHOTOACTIVITY IN VISIBLE LIGHT REGION

TAN WOOI CHUAN, MAKSUDUR RAHMAN KHAN

UNIVERSITY MALAYSIA PAHANG, PAHANG, MALAYSIA, paradise_wc@yahoo.com

Abstract: In recent year, photocatalyst has been gaining a wide attention as the ability to harness the free energy from sunlight to perform variety of function such as organic degradation, solar cell and etc. When used as photocatalyst, titanium dioxide (TiO_2) is able to absorb ultraviolet light only (UV) to initiate the oxidation and reduction which is able to speed up the degradation of dye. This thus provides a cheap and efficient method to solve the dye mismanagement that is face in industries these days. In this work, the titanium dioxide nanoparticle is modified via hydrazine wet method to increase photocatalytic activity. The photocatalytic activity is studied via methylene blue degradation, followed by the kinetic study on the methylene blue degradation. The catalyst has been characterized via UV-VIS spectrophotometer, FTIR machine and XRD machine. From the result, we realized that the main reaction that occurred during the modification is combustion of hydrazine on the surface of TiO_2. From the UV-Vis spectrum, we found out that the modify catalyst can absorb more visible light as compare to the commercial TiO_2. FTIR spectrums indicated that NH_x group, NO group and an increase of OH group is presented after the modification. XRD pattern analysis suggested the crystallinity of the catalyst is slightly increased after the modification. Methylene blue degradation also showed that the modified catalyst have a higher activity as compared to the commercial one. The results obtained suggesting that the photocatalytic activity is increasing due to the ability of the catalyst to absorb visible light after the treatment. The modeling is done by relating the rate of methylene blue degradation with the direct hole attack and the hydroxyl radical attack occurred in the reaction.

Keyword: Photocatalyst, TiO_2, Hydrazine, Visible light, Mathematical Modeling

1.0 Introduction

Large amounts of colored wastewater are generated in industries which use dye such as methylene blue to give the desired color to their product. Still these dye is mismanaged and has been discharged into environment especially river without adequate control, resulting negative impact to the environment and to the human health (Zolinger et al, 1991). The presence of dye in in the natural stream can harm the aquatic life by increasing the toxicity and chemical oxygen demand, and impeding photosynthetic phenomena through reduction of light penetration (Bulut et al, 2006). So far, methods that are used to treat the dye are adsorption, electrocoagulation, ultrasonic decomposition, advance chemical oxidation, nanofiltration, and chemical coagulation followed by sedimentation were implemented to remove dyes from wastewater (Sannino et al, 2013). In recent year photocatalytic degradation with TiO_2 under visible light is gaining

more attention in industry and academic. This is so as this method of treatment is cost effective as compared to method that is used currently; where sophisticated equipment is to be used in order to treat the dye. While with the proposed method, only few things are needed for the treatment: a reactor, a mixer, the catalyst and the sunlight.

Photo-catalyst is one of a kind catalyst which utilizing light to play a part in modify the rates of photo-reaction. Photo-catalyst has the ability to initiate oxidation and reduction process when the light is illuminated on the surface of the catalyst due to the existence of the band gap in the semiconductor, which differ them from the normal catalyst which depending on the adsorption, surface reaction and the desorption of the surrounding molecule to improve rate of reaction. When the electron in the valance band has absorbed photon from a particular wavelength, the electron in the valance band will be excited to the conduction band, leaving a hole in the valance band. Later on, the electrons on the conduction band will move to surface of the catalyst to initiate reduction process, while the holes at the valance band will move to surface to initiate oxidation process. So far semiconductor like TiO_2 is proven better in terms of cost, stability and performance compare to other semiconductor, still the large band gap in TiO_2 (3.2eV) causing the catalyst can absorb only UV light and only can work in near UV range visible light only (Jiang et al, 2012). This cause the application of TiO2 inconvenient and costly as another UV source is needed to enable the function of TiO_2. At the same time, sunlight at the top of Earth's atmosphere consisted of about 50% infrared light, 40% visible light and 10% UV light (Qiang Fu, 2003). So it is desired that TiO_2 is modified to be able to absorb those lights from the sun itself.

In order to create the TiO_2 that is much more active in visible light, one method that is studied the most so far is doping nitrogen into the lattice of TiO_2. So far there are various ways to dope the nitrogen into the lattice of TiO_2 such as sol-gel method, reaction of TiO_2 with N-containing species such as ammonia, urea and etc, plasma treatment method, and oxidation of Ti-N film to TiO_2-N film (Viswanathan et al, 2012) . Still usually all these methods is not cost effective for bulk production as the preparation usually involving sophisticated equipment and high temperature, especially the plasma treatment method involving creation of nitrogen in plasma form at temperature at 400˚C in a plasma chamber (Chen et al, 2007).

So far, wet hydrazine treatment method has been showing a promising way to prepare an N-doped TiO_2 (Li et al, 2007; Selvam et al, 2012). The modification process is done where the TiO_2 powder is immersed in hydrazine hydrate (80%) for 12 hour, filtered and dried with air at 110˚C. The simplicity of the process, the unnecessary of using harsh condition, and the needless of calcination making this treatment interesting as it is possible to convert the lab scale production of this catalyst to a larger scale with a minimum cost. Still the reaction that is occurred during the modification is still not fully understood. Hence in this work, our group is attempt to create N-TiO_2 catalyst and to study the reaction that are occurred in the modification that causing the nitrogen to be doped inside the TiO_2. The efficiency of the catalyst modified is then evaluated using the methylene blue degradation. Later on, a mathematical work on the photocatalytic degradation using the modified catalyst is also done in this work.

2.0 Experimental

2.1 Catalyst preparation

The TiO_2 nanoparticle is modified using the hydrazine wet method. The commercial TiO_2 used is supplied by Shanghai Sunny Scientific Collaboration Co., Ltd from China. 1g of TiO_2 is ultra-sonic with 10ml of hydrazine hydrate (64.5%) for 1hr 30 min, soaked for 12hr, and ultra-sonic for 1hr 30min again. The resulting solution is then filtered and dried

with air at 60˚C, 110˚C, and 170˚C, yielding a yellow colored catalyst as will be discussed later. For each catalyst treated at different temperature, we will be name them N-TiO_2-60, N-TiO_2-110, and N-TiO_2-170 respectively in our discussion later.

2.2 Methylene blue degradation

In a typical experiment run, 0.1g of catalyst was suspended in 50ml 50ppm methylene blue. The dark reaction is run for 2hr to let the catalyst to achieve the adsorption equilibrium, and then the xenon lamp is switched on to supply the visible light to the reaction. This is done as to minimize the effect of catalyst adsorption towards the degradation of methylene blue. The experiment is run in a glass jacketed batch reactor in a black box. The black box is used to isolate the reaction from the surrounding light. The temperature of the reaction is controlled using a water cooling system set at 25˚C. A magnetic stirrer with mixing plate is also included in the reaction to ensure the photocatalyst is suspended in the aqueous solution. Hitachi U-1800 UV-Vis spectrophotometer is used to find the concentration of the methylene blue from the reaction.

2.3 Catalyst characterization

The phase of the catalyst is analyzed using Rigaku Miniflex X-Ray Diffractometer. The X-Ray used in the machine is generated using CuKα radiation with wavelength 1.5418A. The Scherrer equation, $D = 0.89\lambda/\beta\cos\theta$ is employed to find the crystal size, where D is the crystal size, β is full width half maximum (FWHM), and θ is the diffraction angle. The optical properties are studied using the HR2000+ High-resolution Spectrometer. The Perkin Elmer Spectrum 100 model FTIR machine is used to detect the species that is presented in the catalyst.

3.0 Result and Discussion

3.1 UV-Vis absorption spectra

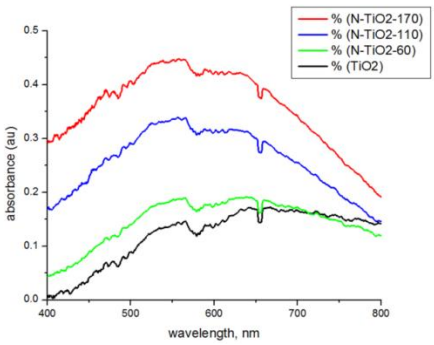

Figure 11: Absorbance spectra of the commercial TiO_2, N-TiO_2-60, N-TiO_2-110, and N-TiO_2-170.

Here the UV-Vis absorption spectrum of the catalyst is studied. From figure 1, it is obvious that in the visible light wavelength (400nm to 700nm), the 170˚C treated band gap is able to absorbed more visible light as compared to the commercial TiO_2. It is also noticed that the visible absorption of the catalyst is increasing when the drying temperature is increasing also. Another property that is change along the increment of temperature is the color of the catalyst. From figure 2, it can be seen that for the treated TiO_2 at 60˚C, the color of the catalyst still remain white. As for the TiO_2 treated at 110˚C, a light yellow yolk color TiO_2 is formed. And when the temperature is further raised to 170˚C, a dirty dark yellow yolk color TiO_2 is created. As for the yellow of the catalyst, it can infer that the nitrogen is successfully doped into the TiO_2 lattice, changing the color of the catalyst from white to yellow (Asahi et al, 2001; Randorn et al, 2010; Li et al, 2007; Selvam et al, 2012). The dirty color at N-170-TiO_2 can be imparted from the presence of OH group in catalyst (Chung et al, 2000; Chen et al, 2011). Another ratiocination that we can make here is that the hydrazine is ignited in the reaction. As the temperature of the oxygen is increase, the combustion is becoming more energetic, thus combust and trap the nitrogen into the TiO_2 lattice.

Taking the basis of the change in color to intense yellow catalyst and the behavior of the UV-Vis spectra for now, we can infer that nitrogen element is doped into the TiO_2 lattice from the hydrazine hydrate, which created the mid-gap in the forbidden band gap that is responsible for the visible light absorption of the catalyst (Asahi et al, 2001). And as the temperature is increasing, more nitrogen is trapped into the TiO_2 lattice due to the more energetic combustion at higher temperature, causing the catalyst to be able to absorb more visible light after modification. From here, due to the time constrain and the financial issue that we faced in the project, we have screened the best catalyst available so far, N-TiO_2-170 to further our discussion.

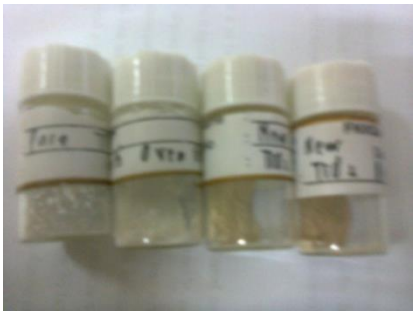

Figure 12: Color of the catalyst after the wet hydrazine treatment. From left: commercial TiO_2, N-TiO_2-60, N-TiO_2-110, and N-TiO_2-170.

3.2 FTIR analysis

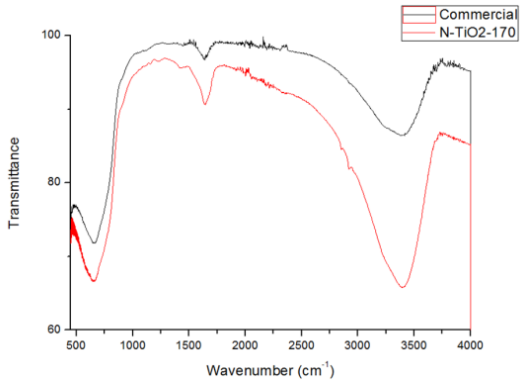

Figure 13: FTIR spectra for the commercial TiO_2 and N-TiO_2-170

Here the FTIR spectra for the treated and the untreated TiO_2 are discussed. Figure 3 shows the FTIR spectra for the commercial TiO_2 and the N-TiO_2-170. From the figure, several peaks that relate to TiO_2 can be observed. The broad band centered at 500-600cm^{-1} is likely due to vibration of Ti-O bonds in TiO_2 lattice (Gao et al, 2003). While the peaks appeared at 1620-1630cm^{-1} and the broad peaks appearing at 3100-3600cm^{-1} are assigned to vibrations of hydroxyl groups (Klingenberg et al, 1996). As in the N-TiO_2-170, these peak that mentioned above overlap with the broad bands of the stretching and deformation modes of NH_x groups (Khabashesku et al, 2000). At the same time, a weak bond is appeared in the modified TiO_2 at 1200-1550cm^{-1} signifying the appearance of nitrogen oxide species (Navio et al, 1996). In the spectra for the 170˚C treated TiO_2, the sharp increase at the peak 1620-1630cm^{-1} and 3100-3600cm^{-1} also might be due to the increase of the isolated hydroxyl group as reported by Chung et al (2000) where the hydroxyl group is restored when the hydrazine gas is interacting with TiO_2 at temperature ranging from 150˚C to 200˚C. Hence, from the FTIR spectra analysis, we can deduce that there are NH_x and few NO species that is appeared TiO_2 after hydrazine treatment. Another deduction can be made is that the increase in the OH functional group is observed after the hydrazine treatment.

3.3 XRD Analysis

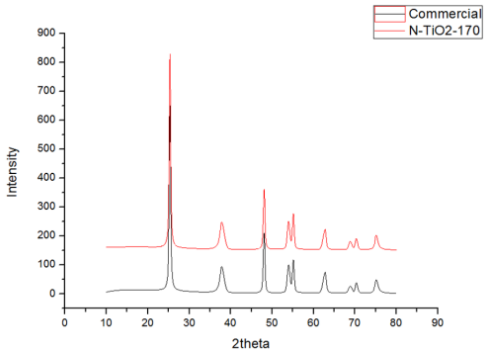

Figure 14: XRD Pattern for commercial TiO_2 and N-TiO_2-170

Here we will be studying the phase of the catalyst via the XRD analysis. The X-Ray diffraction pattern for the commercial TiO_2 and the 170˚C treated TiO_2 are shown in the figure 4.2. From the figure, we can see that there is a main peak at 2θ = 25.32˚ which representing TiO_2 anatase phase. The peak observed at the specific 2θ which at 25.328˚, 37.76˚, 48.07˚, 53.93˚, 55.09˚, 62.83˚, 68.77˚, 70.25˚, and 75.01˚ is the diffraction of the crystal plane of anatase phase at (1,0,1), (1,0,3), (2,0,0), (1,0,5), (2,1,1), (2,1,3), (1,1,6) (2,2,0), and (2,1,5) respectively matching library available and provided by Rigaku XRD desktop. Hence we can confirm that both commercial TiO_2 and the 170˚C treated TiO_2 now is in anatase phase. This show that the method will not change the anatase phase back to the rutile phase again, as in accordance Selvam et al (2012) findings. .

Observing the properties of the main peak of the anatase at 2θ=25.328˚ from figure 4, we can also see that the intensity height of the catalyst is increasing from 647.95 to 671.59 after the commercial TiO_2 is treated at 170˚C. This increment shows that the crystallinity of the treated catalyst is slightly improved as compared to the commercial one. This founding is in parallel with Li et al (2003) XRD analysis result, where the intensity of the peak is increased significantly at anatase crystal plane after thy hydrazine wet treatment method.

The size of the crystallite for both commercial TiO_2 and N-TiO_2-170 is also studied from the XRD pattern. Size of the crystal is important as the size will affect the band gap of the semiconductor directly also. As the size of crystal is small, the band gap of the semiconductor will be larger due to the quantum size effect (Dong et al, 2007). From the Scherrer equation, the size of the crystal at 2θ= 25.328˚ for both commercial TiO_2 and N-TiO_2-170 is 19.426nm and 19.561nm respectively. This slight shift in the size of crystal is also evidence as modified catalyst can absorb visible light, signifying that the band gap of the crystal has been lowered due to the slight increase in the size of the crystal.

3.4 Methylene Blue Degradation

As from the table above, we can see there is not much change on the adsorption of the catalyst before and after the hydrazine treatment. Still this is not our main focus as we are more interested in the photoactivity of the catalyst now. As can be seen from figure 4.8, as the time goes, the methylene blue is degrading much faster when the 170˚C treated catalyst is used as compared to the commercial catalyst. Since so far the main difference between the commercial catalyst and the N-TiO_2-170 catalyst is that the treated catalyst can absorb more visible light as compare to the untreated one, we deduced that this absorption of the visible light is responsible for the increase in photoactivity of the catalyst itself. When more light is being absorb into the catalyst, more electrons are excited from the valance band to the conduction band, thus producing more holes that is responsible for the direct holes attack and the hydroxyl radical production as we are using the reaction pathway that is suggested by Sivalingam et al (2003).

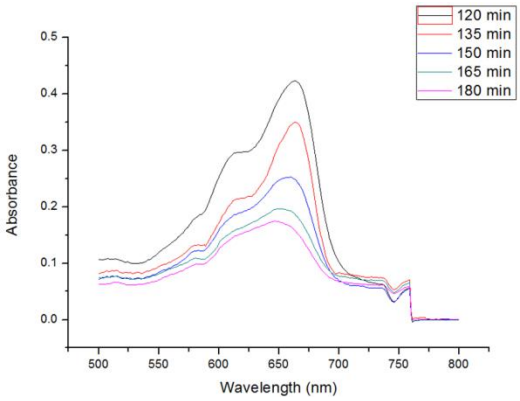

Figure 15: UV-Vis spectra for methylene blue collected from reaction with commercial TiO_2 at various time

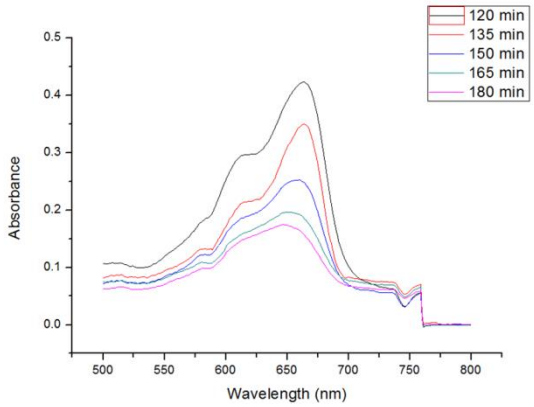

Figure 16: UV-Vis spectra for methylene blue collected from reaction with N-TiO_2-170 at various time

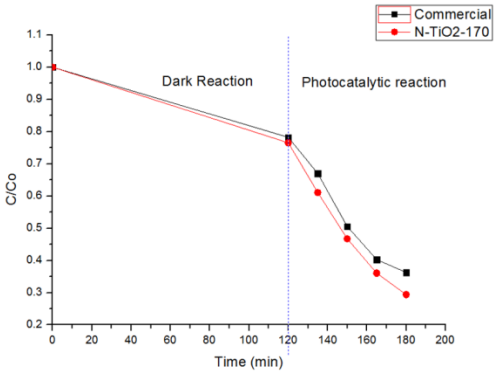

Figure 17: Degradation of methylene blue with commercial TiO_2 and N-TiO_2-170; Initial methylene blue concentration: 50ppm; Weight of catalyst: 0.01g

3.5 Kinetic Studies

Here the reaction modeling is done for the reaction with N-TiO_2-170. The model that we used is the modeling considering the direct hole attack and the hydroxyl radical attack as proposed by Sivalingam et al (2003).

First the hole generation will be discussed. In the reaction, the hole is mainly generated from the excitation of electron from the valance band to conduction band, where the hole is left in the valance band after electron is excited as shown below:

$$TiO_2 + h\nu \xrightarrow{k_e} h_{VB}^{+} + e_{CB}^{-} \qquad E.1$$

The k_e is the reaction constant for this reaction.

At the same time, the holes produced will also undergo recombination of electrons again to generate the heat back as shown below:

$$h_{VB}^{+} + e_{CB}^{-} \xrightarrow{k_{rc}} heat \qquad E.2$$

The k_{rc} is the reaction constant for this reaction.

Later on, the hole generated will directly attack either the dye adsorbed on the surface of the catalyst, or the unbounded dye in the solution to yield the cationic dye radicals. And the radicals produced will further react to get the end species as shown below:

$$S - D + h_{VB}^{+} \xrightarrow{k_{hr}^{a}} S - D^{0+} \rightarrow \text{end species} \qquad E.3$$

$$D + h_{VB}^{+} \xrightarrow{k_{hr}^{b}} D^{0+} \rightarrow \text{end species} \qquad E.4$$

The k^{a}_{hr} and k^{b}_{hr} is the reaction constant for both reactions respectively; S-D is the dye adsorbed on the catalyst surface; D is the unbounded dye in the solution; and D^{0+} is the cationic radical dye generated by direct hole attack.

Next the hydroxyl radical generation will be discussed. The hydroxyl radical can be generated via the attack of hole on the hydroxyl group or the water adsorbed on the surface of the catalyst as shown below:

$$S - H_2O + h_{VB}{}^+ \underset{k'_{tr}}{\overset{k_{tr}}{\rightleftharpoons}} S - \dot{O}H + H^+ \quad \text{E.6}$$

$$S - OH^- + h_{VB}{}^+ \underset{k'_{tr}}{\overset{k_{tr}}{\rightleftharpoons}} S - \dot{O}H \quad \text{E.}$$

The k_{tr} and k'_{tr} is the reaction constant for the forward and backward reaction of both reversible reactions. S-OH^- is the anionic hydroxyl group that adsorbed on the catalyst surface. S-H_2O is the water group that is adsorbed on the catalyst surface. And S-OH· is the hydroxyl radical produced that is adsorbed on the surface.

Later, the adsorption and desorption of the mobile species in the reaction will be discussed. Here hydroxyl and dye can be adsorbed and desorbed away from surface of the catalyst as shown below:

$$S + D \underset{k'_D}{\overset{k_D}{\rightleftharpoons}} S - D, \quad K_D = \frac{k_D}{k'_D} \quad \text{E.7}$$

$$S + \dot{O}H \underset{k'_{OH}}{\overset{k_{OH}}{\rightleftharpoons}} S - \dot{O}H, \quad K_{OH} = \frac{k_{OH}}{k'_{OH}} \quad \text{E.8}$$

The k_D and k'_D is the reaction constant for the forward and backward reaction for E.8. And K_D is the equilibrium constant for the reaction E.7. While the k_{OH} and k'_{OH} is the reaction constant for the forward and backward reaction for E.8. And K_{OH} is the equilibrium constant for the reaction E.8

In the solution, since now both dye and hydroxyl radical is available either on catalyst surface or in the bulk, four possible combinations has been proposed where the reaction can occur: a) bounded hydroxyl radical and bounded dye; b) bounded hydroxyl radical and unbounded dye; c) unbounded hydroxyl radical and bounded dye; d) unbounded hydroxyl radical and unbounded dye as shown below:

Case (a):

$$S - D + S - \dot{O}H \xrightarrow{k_r^a} S + S - D'^0 + M^+OH^- \quad \text{E.9}$$

Case (b):

$$D + S - \dot{O}H \xrightarrow{k_r^b} S + D'^0 + M^+OH^- \rightarrow \text{end species} \quad \text{E.10}$$

Case (c):

$$S - D + \dot{O}H \xrightarrow{k_r^c} S - D'^0 + M^+OH^- \rightarrow \text{end species} \quad \text{E.11}$$

Case (d):

$$D + \dot{O}H \xrightarrow{k_r^d} D'^0 + M^+OH^- \rightarrow \text{end species} \quad \text{E.12}$$

The k_r^a, k_r^b, k_r^c, k_r^d is the reaction constant for each reactions respectively. D'^0 is the cationic dye radical formed by hydroxyl radical attack. While the M^+ is the cation released from the dye molecule after being attack by hydroxyl radical.

Later on, relating the rate of disappearance of methylene blue to the direct hole attack mechanism (E.3 and E.4) and hydroxyl radical attack (E.9, E.10, E.11, E.12):

$$\begin{aligned} -r_D = {} & k_{hr}^a[S - D][h_{VB}{}^+] + k_{hr}^b[D][h_{VB}{}^+] \\ & + k_r^a[S - D][S - \dot{O}H] + k_r^b[D][S - \dot{O}H] \\ & + k_r^c[S - D][\dot{O}H] + k_r^d[D][\dot{O}H] \end{aligned} \quad \text{E.13}$$

In order to define E.13 in a measurable parameter [D], several concentration formulas have been formulated out. From E.7 and E.8, the concentration of [S-D] and [S-ȮH] is further defined as follows:

$$[S - D] = K_D[S][D] \quad \text{E.14}$$

$$[S - \dot{O}H] = K_{OH}[S][\dot{O}H] \quad \text{E.15}$$

As to redefine [ȮH], a total hydroxyl radical balance has been done

from E.5, E.6, E.9, E.10, E.11, and E.12 as follows:

$$\begin{aligned}\frac{d([\dot{O}H]+[S-\dot{O}H])}{dt} &= k_{tr}[S-OH^-][h_{VB}{}^+] - k'_{tr}[S-\dot{O}H] \\ &+ k_{tr}[S-H_2O][h_{VB}{}^+] - k'_{tr}[S-\dot{O}H][H^+ \\ &- k_r^a[S-\dot{O}H][S-D] - k_r^b[S-\dot{O}H][D] \\ &- k_r^c[\dot{O}H][S-D] - k_r^d[\dot{O}H][D]\end{aligned}$$

It is well known that normally in a batch reaction, the reaction is normally pccured in unsteady state manner. Still as to ease our calculation at this stage, a quasi-steady state assumption (QSSA) is made as to further evaluating E.16:

$$\frac{d([\dot{O}H]+[S-\dot{O}H])}{dt} = 0$$

$$[\dot{O}H] = \frac{k_{tr}\{[S-OH^-]+[S-H_2O]\}[h_{VB}{}^+]}{K_{OH}\{k'_{tr}(1+[H^+])[S]+k_r^a[S-D][S] + k_r^b[D][S]\}+k_r^c[S-D]+k_r^d[D]} \quad \text{E.17}$$

As to redefine [h^+_{VB}], a hole concentration balance is also done from E.1, E.2, E.5, and E.6 as follows:

$$\begin{aligned}\frac{d[h_{VB}{}^+]}{dt} &= k_e[S] - k_{rc}[e_{CB}{}^-][h_{VB}{}^+] \\ &- k_{tr}[S-OH^-][h_{VB}{}^+] + k'_{tr}[S-\dot{O}H] \\ &- k_{tr}[S-H_2O][h_{VB}{}^+] \\ &+ k'_{tr}[S-\dot{O}H][H^+]\end{aligned} \quad \text{E.18}$$

Here, by assuming that the recombination process (E.2) is happening at faster rate as compared to other reaction and applying QSSA for E.18, E.18 can be further redefine to:

$$\frac{d[h_{VB}{}^+]}{dt} = 0$$

$$[h_{VB}{}^+] = \sqrt{\frac{k_e[S]}{k_{rc}}} \quad \text{E.19}$$

Substituting E.14, E.15, E.17 and E.19 back into E.13, we will be getting:

$$-\frac{d[D]}{dt} = k_{0h}[D] + \frac{k_0 K_0[D]}{1+K_0[D]} \quad \text{E.20}$$

With the following constant that has been define along the substitution:

$$k_{0h} = k^a_{dch} + k^b_{dch}$$

$$k_0 = k_{dc} \quad \text{and} \quad K_0 = K^a_{DC} + K^b_{DC} + K^c_{DC} + K^d_{DC}$$

Parameters	Expressions
k^a_{dch}	$k^a_{hr} K_D[S]\sqrt{\frac{k_e[S]}{k_{rc}}}$
k^a_{dch}	$k^b_{hr}\sqrt{\frac{k_e[S]}{k_{rc}}}$
k_{dc}	$k_{tr}\{[S-OH^-]+[S-H_2O]\}\sqrt{\frac{k_e[S]}{k_{rc}}}$
K^a_{DC}	$\frac{k^a_r K_D[S]}{k'_{tr}(1+[H^+])}$
K^b_{DC}	$\frac{k^b_r}{k'_{tr}(1+[H^+])}$
K^c_{DC}	$\frac{k^c_r K_D}{K_{OH}k'_{tr}(1+[H^+])}$
K^d_{DC}	$\frac{k^d_r}{K_{OH}k'_{tr}(1+[H^+])}$

Here the k_{0h} is the overall rate constant for direct hole attack, k_0 is the overall rate constant for hydroxyl radical attack. Both constant is dependent on the reaction conditions and the catalyst properties, but they are independent of the nature of the dye used. K_0 is the adsorption equilibrium constant dependent on the characteristic of dye and the rate –determining step.

Considering the effect of the intermediate along the reaction, E.20 is further defined as follows:

$$\frac{-1}{r_{Dt}} = \frac{1}{K_0(\frac{k_{0h}}{K_0} + k_0)} \frac{1}{[D]_t} + \frac{1}{\frac{k_{0h}}{K_0} + k_0}$$

Here r_{Dt} is the rate of degradation of the methylene blue at specific time. And $[D]_t$ is the concentration of the methylene blue at the specific time.

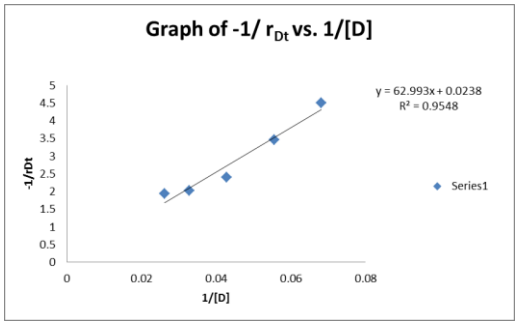

Figure 18: Graph of -1/rate of methylene blue degradation versus the 1/concentration of the methylene blue

From figure 4.10, the fitted linear equation obtained is y=51.309x + 0.3876. This fitted equation is acceptable as the R^2 obtained as a result of fitting is above 0.95. Hence, comparing the model equation and the fitted linear equation from figure 4.10, we obtained (k_{0h}/K_0+k_0) = 42.012 mg L^{-1} min^{-1}, while K_0=3.78x10^{-4}L mg^{-1}. According to Sivalingam et al (2003), the higher value of K_0 implies the blocking of the active sites of the catalyst due to strong adsorption, while the higher value of (k_{0h}/K_0+k_0) indicating the higher degradation rates of the dye.

4.0 Conclusion

In conclusion, a visible light active TiO_2 is successfully modified by wet hydrazine method. The visible light absorption can be origin from the presence of NH_x group and NO group in the catalyst, which giving mid gap state which reduce the amount of energy needed to excite the electron. In other word, the band gap of the catalyst is reduced as crystal size is increasing after modified. The main reaction that occurred during the modification is the combustion of hydrazine which ignited and trapped the N species into TiO_2 lattice. The crystallinity of the catalyst is also increase after modification which is beneficial to the photoactivity of the reaction. With all those properties modified, the photoactivity of the methylene blue degradation is improved after the modification. The modeling is developed based on the relationship of the methylene blue degradation with direct hole attack and hydroxyl radical attack to explain the experimental data.

References

Asahi, R., Morikawa, T., Ohwaki, T., Aoki, K., & Taga, Y. (2001). Visible-Light Photocatalysis in Nitrogen-Doped Titanium Oxides. *Science, 293*(5528), 269-271. doi: 10.1126/science.1061051

Beranek, R., & Kisch, H. (2008). Tuning the optical and photoelectrochemical properties of surface-modified TiO2. [10.1039/B711658F]. *Photochemical & Photobiological Sciences, 7*(1), 40-48. doi: 10.1039/b711658f

Chen, C., Bai, H., Chang, S.-m., Chang, C., & Den, W. (2007). Preparation of N-doped TiO2 photocatalyst by atmospheric pressure plasma process for VOCs decomposition under UV and visible light sources. *Journal of Nanoparticle Research, 9*(3), 365-375. doi: 10.1007/s11051-006-9141-2

Chen, X., Liu, L., Yu, P. Y., & Mao, S. S. (2011). Increasing Solar Absorption for Photocatalysis with Black Hydrogenated Titanium Dioxide Nanocrystals. *Science, 331*(6018), 746-750. doi: 10.1126/science.1200448

Chuang, C.-C., Shiu, J.-S., & Lin, J.-L. (2000). Interaction of hydrazine and ammonia with TiO2. [10.1039/B001389G]. *Physical Chemistry Chemical Physics, 2*(11), 2629-2633. doi: 10.1039/b001389g

Fu, Q. (2003). Radiation (SOLAR). In R. H. Editor-in-Chief: James (Ed.),

Encyclopedia of Atmospheric Sciences (pp. 1859-1863). Oxford: Academic Press.

Gao, Y., Masuda, Y., Peng, Z., Yonezawa, T., & Koumoto, K. (2003). Room temperature deposition of a TiO2 thin film from aqueous peroxotitanate solution. [10.1039/B208681F]. *Journal of Materials Chemistry, 13*(3), 608-613. doi: 10.1039/b208681f

Jiang, Z., Xiao, T., Kuznetsov, V. L., & Edwards, P. P. (2010). Turning carbon dioxide into fuel. *Philosophical Transactions of the Royal Society A: Mathematical, Physical and Engineering Sciences, 368*(1923), 3343-3364. doi: 10.1098/rsta.2010.0119

Khabashesku, V. N., Zimmerman, J. L., & Margrave, J. L. (2000). Powder Synthesis and Characterization of Amorphous Carbon Nitride. *Chemistry of Materials, 12*(11), 3264-3270. doi: 10.1021/cm000328r

Kim, D. S., & Kwak, S.-Y. (2007). The hydrothermal synthesis of mesoporous TiO2 with high crystallinity, thermal stability, large surface area, and enhanced photocatalytic activity. *Applied Catalysis A: General, 323*(0), 110-118. doi: http://dx.doi.org/10.1016/j.apcata.2007.02.010

Klingenberg, B., & Vannice, M. A. (1996). Influence of Pretreatment on Lanthanum Nitrate, Carbonate, and Oxide Powders. *Chemistry of Materials, 8*(12), 2755-2768. doi: 10.1021/cm9602555

Li, D., Huang, H., Chen, X., Chen, Z., Li, W., Ye, D., & Fu, X. (2007). New synthesis of excellent visible-light TiO2−xNx photocatalyst using a very simple method. *Journal of Solid State Chemistry, 180*(9), 2630-2634. doi: http://dx.doi.org/10.1016/j.jssc.2007.07.009

Navio, J. A., Cerrillos, C., & Real, C. (1996). Photo-induced Transformation, upon UV Illumination in Air, of Hyponitrite SpeciesN2O22- Preadsorbed onTiO2 Surface. *Surface and Interface Analysis, 24*(5), 355-359. doi: 10.1002/(sici)1096-9918(199605)24:5<355::aid-sia122>3.0.co;2-d

Randorn, C., & Irvine, J. T. S. (2010). Synthesis and visible light photoactivity of a high temperature stable yellow TiO2 photocatalyst. [10.1039/C0JM01370F]. *Journal of Materials Chemistry, 20*(39), 8700-8704. doi: 10.1039/c0jm01370f

Sannino, D., Vaiano, V., Sacco, O., & Ciambelli, P. (2013). Mathematical modelling of photocatalytic degradation of methylene blue under visible light irradiation. *Journal of Environmental Chemical Engineering, 1*(1–2), 56-60. doi: http://dx.doi.org/10.1016/j.jece.2013.03.003

Selvam, K., & Swaminathan, M. (2012). Nano N-TiO2 mediated selective photocatalytic synthesis of quinaldines from nitrobenzenes. [10.1039/C2RA01178F]. *RSC Advances, 2*(7), 2848-2855. doi: 10.1039/c2ra01178f

Sivalingam, G., Nagaveni, K., Hegde, M. S., & Madras, G. (2003). Photocatalytic degradation of various dyes by combustion synthesized nano anatase TiO2. *Applied Catalysis B: Environmental, 45*(1), 23-38. doi: http://dx.doi.org/10.1016/S0926-3373(03)00124-3

Viswanathan, B., & Krishanmurthy, K. R. (2012). Nitrogen Incorporation in TiO2: Does It Make a Visible Light Photo-Active Material? *International Journal of Photoenergy, 2012*, 10. doi: 10.1155/2012/269654

Zollinger, H. (1992). Color Chemistry as Reflected in Helvetica Chimica Acta. *Helvetica Chimica Acta, 75*(6), 1727-1754. doi: 10.1002/hlca.19920750602